

The Potential for diffusing Copper into Tourmaline

Preparation for initial experimentation

Sudarat Saeseaw and Kenneth Scarratt
GIA Laboratory, Bangkok

John L. Emmett
Crystal Chemistry, Brush Prairie, Washington

(Updated July 27th, 2009)

Introduction

There has been some discussion within the gemological community concerning the possibility that some tourmaline on the market particularly those from Mozambique, may have been diffused with Cu (James, 2009a, James, 2009b, James, 2009c)¹. While the authors and their colleagues have not observed any characteristics that might lead them to believe that such a situation exists in the market today (e.g., see (Koivula J. I., 2009, Koivula, 2009, Wise, 2009), Wise, 2009), as Paraíba tourmaline (LMHC, 2007)² is a commercially important gem material it was felt that some experimental gemology to investigate the feasibility of such a treatment was required.

¹ For a detailed description of diffusion processes see Emmett, J. L., Scarratt, K., F. McClure, S., Moses, T., Douthit, T.R., Hughes, R., Novak, S., Shigley, J.E., Wang, W., Bordelon, O., Kane, R.E. (2003) Berillium Diffusion of Ruby and Sapphire. *Gems & Gemology*. 39. 2. available at http://www.giathai.net/pdf/Beryllium_G&G_2003-02.pdf.

² A blue (electric blue, neon blue, violet blue), bluish green to greenish blue or green elbaite tourmaline, of medium to high saturation and tone, mainly due to the presence of copper (Cu) and manganese (Mn).

Over the last few months an assortment of tourmaline has been acquired. The stones have been analyzed, sorted and selected (Figure 1) for the copper diffusion experiments. These experiments are presently underway (March 2009) and are being carried out by Crystal Chemistry located in Brush Prairie, WA. Details of these experiments and their results will be available and published once complete.

Pre-treatment Examination

For this study a total of 30 faceted blue, green, blue-green, and violet samples have been examined; all are tourmaline and stated to be from Mozambique (Figure 1).

Standard gemological properties including refractive index (RI), specific gravity (SG), and UV fluorescence have been determined for each stone and in addition UV-Vis-NIR, IR, Raman and LA-ICP-MS analyses have been recorded (Abduriyim, 2006).



Figure 1: Thirty tourmalines selected for diffusion experiments seen here before treatment.

Standard gemological properties

Refractive indices for the group were determined to be in the ranges $n_o = 1.639-1.642$, and $n_e = 1.619-1.620$, with birefringence being $= 0.019-0.021$. The SGs were determined to be between $3.04 - 3.08$. Under UV radiation the stones were inert to faint blue in LWUV and inert in SWUV.

Microscopic characteristic

All samples exhibited typical tourmaline inclusions. These included trichites (Laurs, 2008), irregular and partially healed fissures (Figure 2, Figure 3 and Figure 5) and parallel channels (Figure 4 and Figure 5). Some were cracked and some of these cracks were frosty in appearance.



Figure 2: Partially healed fissures in one of the tourmaline selected for diffusion experiments.



Figure 3: Partially healed fissures in one of the tourmaline selected for diffusion experiments.

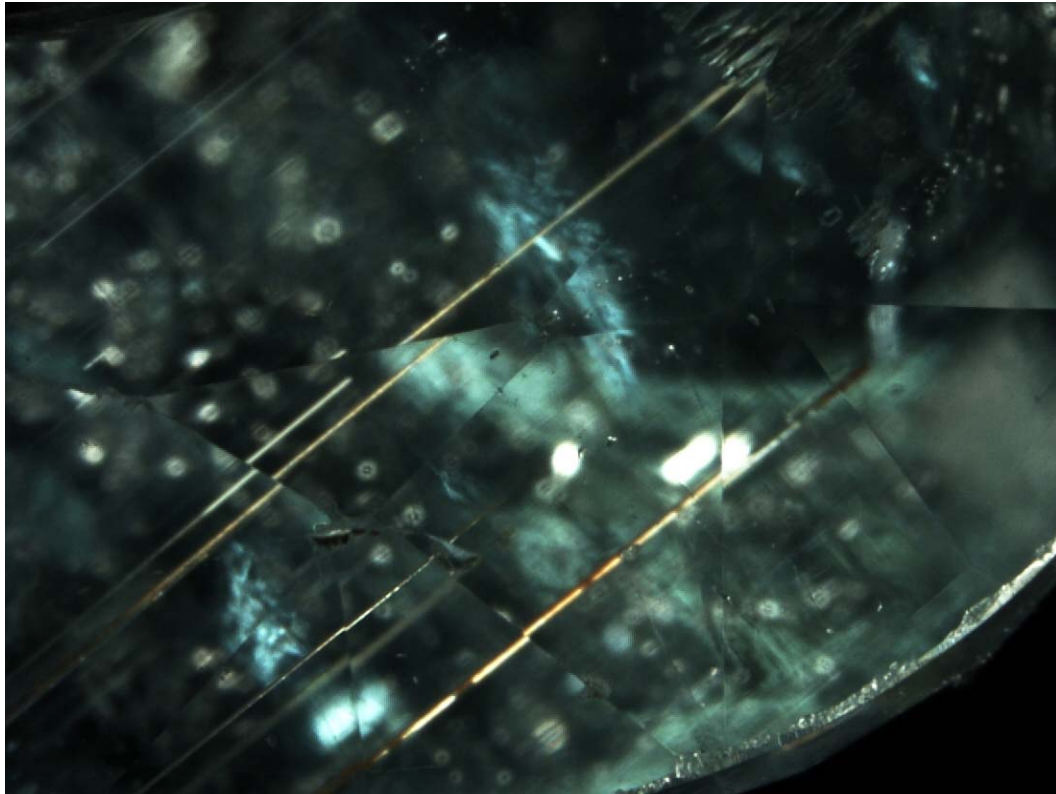


Figure 4: Yellow and red-brown hollow tubes in one of the tourmaline selected for diffusion experiments

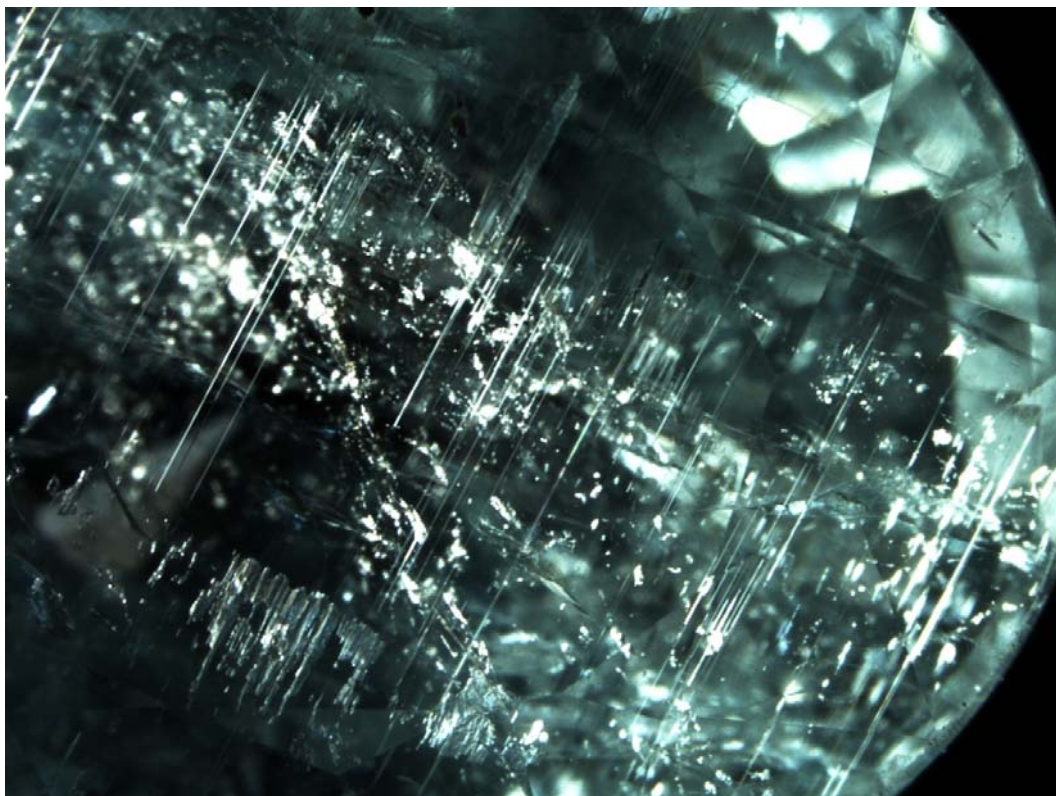


Figure 5: Partially healed fissures and parallel growth tubes arrange in same direction in one of the tourmaline selected for diffusion experiments

UV-Vis-NIR spectroscopy

UV-Vis-NIR absorption spectra displayed a very weak but sharp peak at about 415nm and broad band at about 515 nm, which are attributed to Mn^{2+} and Mn^{3+} , respectively (Fritsch, *et al.*, 1990). Two different spectra types were found in the group. The first (Figure 6) recorded broad bands at approximately 695 and 920nm that are attributed to Cu (Fritsch, *et al.*, 1990). The maxima are located at about 690 and 900nm in the $E \perp C$ direction and about 740 and 940nm in the $E // C$ direction. The second (Figure 7) recorded a broad band with a maximum at about 720nm, assigned to intervalence charge transfer $Fe^{2+} \leftrightarrow Fe^{3+}$ (Fritsch, *et al.*, 1990). Both types of tourmaline spectra showed sharp bands in the near infrared between 1400 and 1500nm that are assigned to O-H stretching vibrations (Fritsch, *et al.*, 1990).

IR spectroscopy

Infrared spectra recorded for all samples were the same (Figure 8). The spectra are characterized by broad bands at about 7593, 7120, 6993, 6775 cm^{-1} which are attributed to hydroxyl (O-H) stretching and 4599, 4538, 4439, 4345, 4212, 3909 cm^{-1} which are attributed to M-OH bonding where M maybe Al, Fe, Mn, etc (Reddy, 2007).

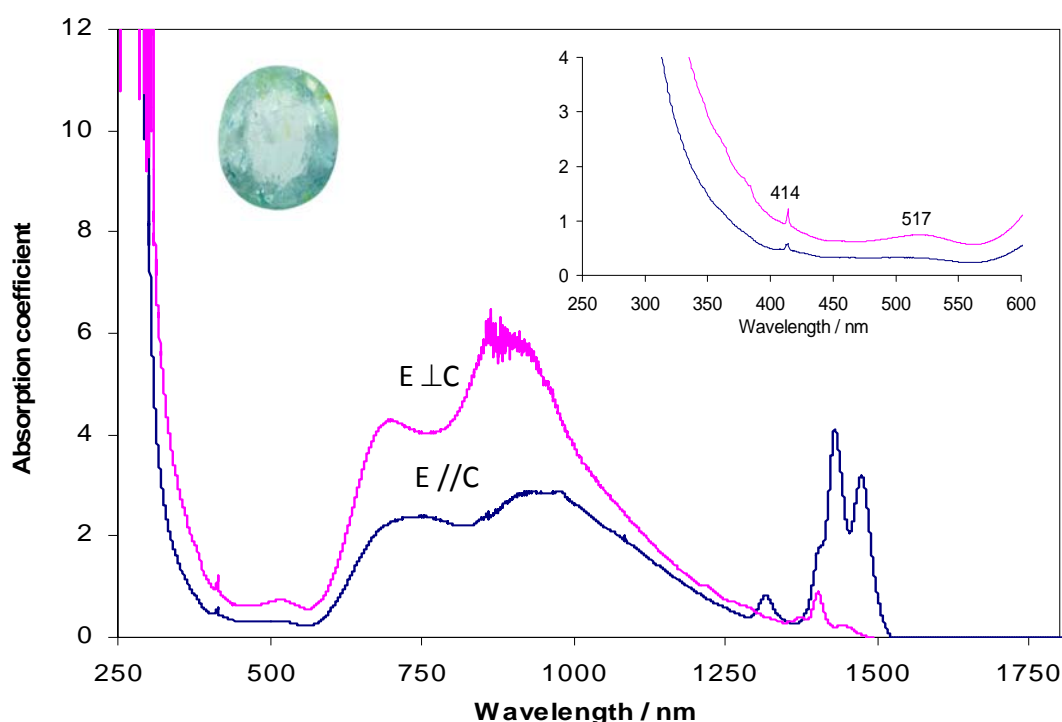


Figure 6: An example of the first of two types of UV-Vis-NIR spectra noted for this group of 30 tourmaline. The FeO concentration of this sample is 105.6 ppmw.

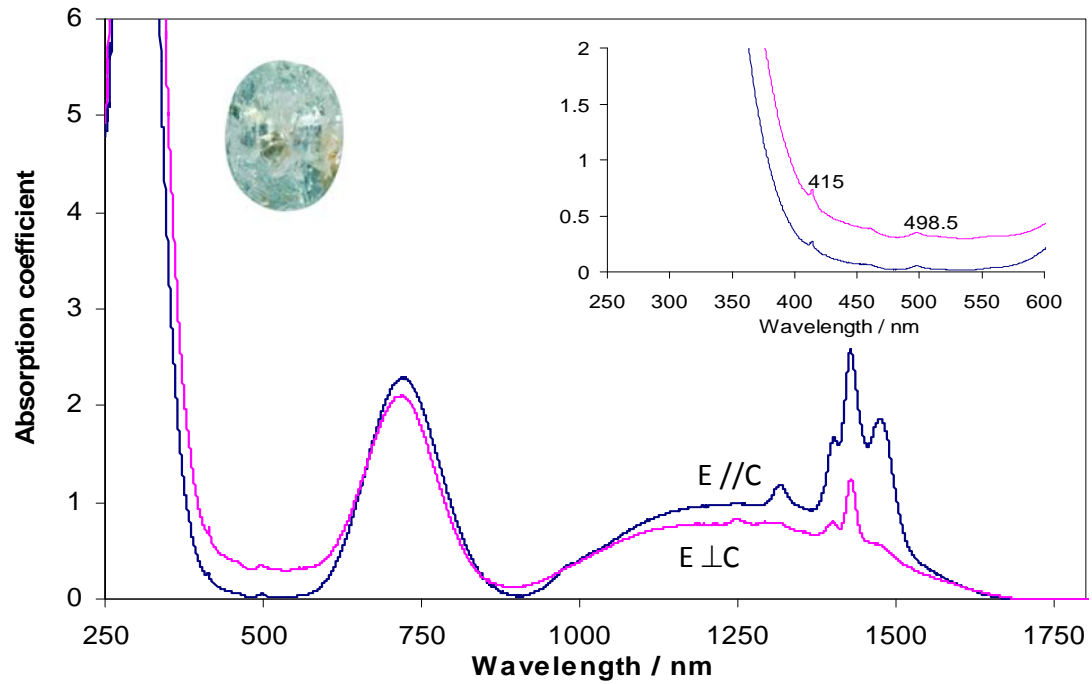


Figure 7: An example of the second of two types of UV-Vis-NIR spectra noted for this group of 30 tourmaline. FeO concentration of this sample is 7222.9 ppmw.

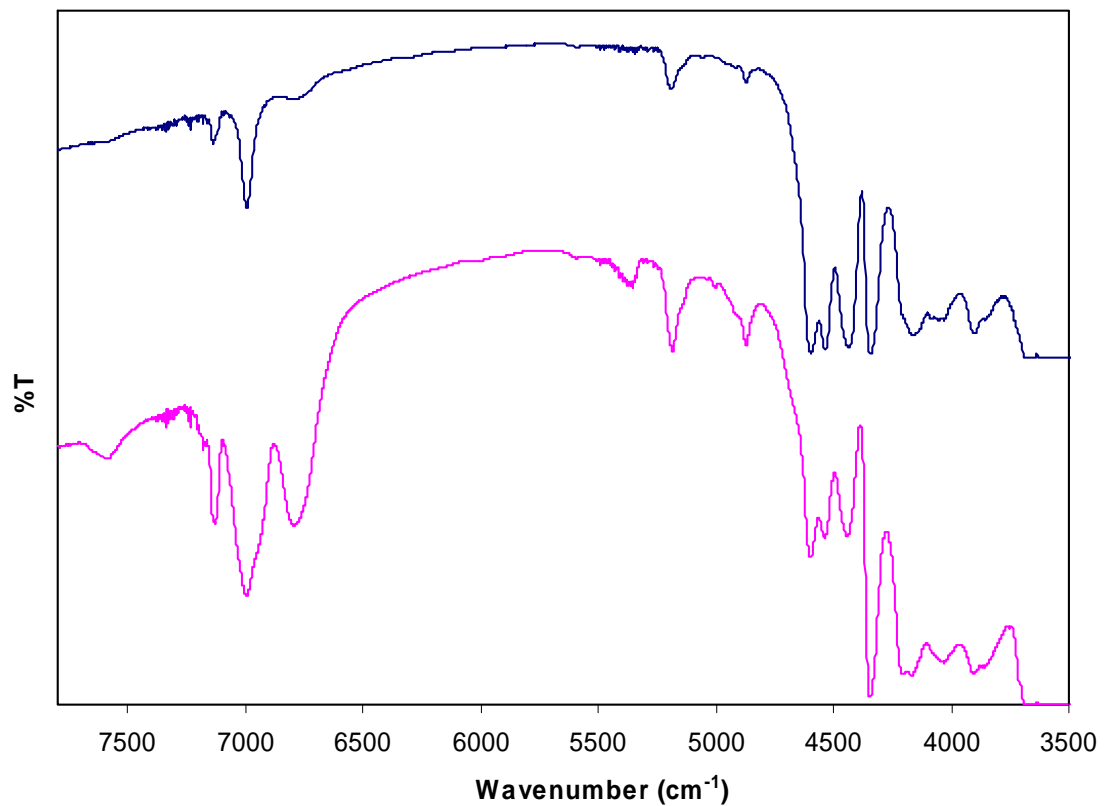


Figure 8: Examples of the infra-red spectra common to all 30 tourmaline samples.

Laser-ablation inductively coupled plasma mass spectrometry (LA-ICP-MS)

A New Wave UP-213 laser-ablation coupled with a Thermo X series II ICP-MS was used to obtain the full chemistry of all 30 samples (Figure 1). The laser-ablation parameters were; 40um spot diameter, ~10 J/cm² laser fluence, 7 Hz repetition rate, and 25 second dwell time. NIST 610 and 612 glass reference material were used to calibrate and boron was used as internal standard. Boron was assumed as 3.26% for all tourmaline in this study. All tourmaline were elbrite with 0.13-0.46 wt% CuO (1076.8 to 3636 ppmw of Cu) and 0.21-2.62 wt% MnO (1631.2 to 20260 ppmw of Mn) with the exception of two samples that did not contain Cu. In this study, most of violetish blue tourmalines have no Fe concentration while some (but not all) green tourmalines do have Fe content.

The process:

A process has now begun which will culminate in an attempt to diffuse some of the stones described here with Cu. Once the various stages of this process are complete the individual stones will be examined and their data collected once more. The before and after data will be compared and presented as progress is made. However, and firstly, to do diffusion type experiments with a new gemstone, there are three necessary steps, see Table 1.

Table 1: The four steps of a diffusion experiment

Step 1
Take some pieces and heat them to various temperatures to see how high a temperature one can heat the stone without damage such as shattering, decomposition, etc.
Step 2
Imbed the stones in various oxide powders (Al ₂ O ₃ , ZnO, ZrO ₂ , MgO, etc.) and heat to the maximum safe temperature determined in step 1, for about 50 hours. Then determine which powder can be used by seeing which powder does not chemically react with the gemstone.
Step 3
Mix -300 mesh copper metal powder or copper oxide powder into the oxide chosen in step 2, and heat at the temperature determined in step 1 for 150 to 200 hours.
Step 4
Cut and polish the stones in cross section and look for evidence of diffusion.

Initial experiments involving step 1 and step 2 have been carried out on the first 15 stones (which usually damages the stones). With these stones have been included some additional (to those in Figure 1) light pink, some yellow and some Paraiba colored tourmaline. The overall results from step 1 are as follows.

The pink tourmaline becomes colorless at both 700 and 800°C and shows no damage; the yellow tourmaline becomes a dark gold brown color at 700 and 800°C, again without damage; whereas the Paraiba colored tourmaline seems to develop

(or become more apparent) a large number of internal fractures at both 800 and 700°C. What is interesting is that some of the fractures show a copper colored 'residue', even though no copper was involved except that naturally in the stone. These fractures are detailed in the section below in text and images.

We are currently running experiments at lower temperatures to find some point at which the material does not fracture but still facilitates the diffusion of Cu and possible other elements. The Paraíba type tourmalines are usually heated to about 545°C to develop good color, so that temperature should be safe except for fracturing by fluid inclusions.

A microscopic view of the effects produced by heating selected tourmalines at 700°C in air for 10 and 100 hours.

As indicated earlier, it appeared that some of the fractures in the heated Paraíba colored tourmaline show a copper colored 'residue' after heating; even though no additional copper was involved in the process except that which was naturally in the stones. To examine this phenomenon further, several additional stones of the same type were selected for further heating. The first group of four being heated under similar conditions to the pre-runs and the second group of four for an increased run time.

The following describes stones 0668225902 (Figure 9), 0668227002 (Figure 12), 0668227202 (Figure 20) and 0668228402 (Figure 29) after being heated in air at 700°C for **10 hours**; and then stones 0668227502 (Figure 44), 0668227702 (Figure 53), 0668228002 (Figure 63) and 0668226602 (Figure 69) after being heated in air at 700°C for **100 hours**.

For all stones there appeared to be a difference in face-up color appearance after heating; stone 0668225902 (Figure 9) appeared bluish green before heating while after its appearance had changed to be more towards purple (Figure 10), a change that could be associated with a more intense and greater distribution of a yellow brown material within some fractures and being reflected within others.

Stone 0668227002 (Figure 12) appeared green before heating and was quite purple afterwards (Figure 13); as before most of the perceived new color could be associated with material within fractures. However, some diffuse purple color gives the impression of coming from within the stone adjacent to, as well as being within, the fractures (Figure 16 and Figure 17).

Stone 0668227202 (Figure 20) appeared to have a purplish tint before heating that seemed more intense afterwards (Figure 21). Again the increase in intensity appeared to arise in the main from the emergence of brown matter within fractures in addition to a change in color (from yellow to reddish brown) of material within some fractures and channels (Figure 25, Figure 26 and Figure 27).

Stone 0668228402 (Figure 29) appeared bluish green before heating while after its color appearance had changed to be more towards purple (Figure 30). The change in appearance appeared to arise again in the main from the emergence of reddish brown matter within fractures in addition to a change in color (from yellow to reddish brown) of material within some fractures and channels (Figure 31, Figure 32, Figure 33, Figure 34, Figure 35 and Figure 36). However, some diffuse reddish brown color again gives the impression of coming from within the stone adjacent to, as well as being within, the fractures (Figure 40, Figure 41, Figure 42 and Figure 43).

These changes in color appearance may to some extent be explained by the probable conversion of the preexisting limonite (yellow) within some fractures and channels into hematite (dark red brown). Raman spectra taken of the content of fractures after heating were characteristic of hematite. The process is explained in papers written by Robert Kammerling and John Koivula (Koivula, 1987, Kammerling, *et al.*, 1989) as follows –

“Limonite is a general term for hydrous cryptocrystalline iron oxides consisting mainly of goethite [α -FeO (OH)] and lepidocrocite [γ -FeO (OH)] with variable absorbed water. Heating of the earthy yellow limonite causes a gradual dehydration (Palache, 1944) that starts at 100°C with the loss of excess water from the limonite. It continues with the conversion of the goethite and lepidocrocite in the limonite to dark red-brown hematite (α -Fe₂O₃), following the formula $2\text{FeO (OH)} + \text{heat (400}^\circ\text{C)} \rightarrow \text{Fe}_2\text{O}_3 + \text{H}_2\text{O}$, with a resulting additional loss of water”.

Clearly the Kammerling and Koivula explanations of the color change process explain the fundamental changes in appearance of the tourmaline samples when heated under the conditions described here. However, the changes in color appearance are rather striking; see for example Figure 10, Figure 13 and Figure 30. Certainly, and contributing to the effect, it would appear that the limonite present in some fissures and within channels becomes mobile within the environment used at 700°C. This can be assumed by the change in color observed in fractures which did not (noticeably) contain limonite prior to heating, e.g., the fracture depicted in Figure 18 and Figure 19.

Further, after the 10 hour run there appeared to be some purple color ‘bleeding’ into the host tourmaline from the colored channels and fractures. This ‘bleeding’ observation was not particularly clear but prompted a second run with a further four stones, but this time at 100 hours.

Stones 0668227502 (Figure 44), 0668227702 (Figure 53), 0668228002 (Figure 63) and 0668226602 (Figure 69) were heated in air at 700°C for **100 hours**. Again, no additional elements were added to the process.

After heating for 100 hours the face-up color appearance of stone 668227502 (Figure 44) considerably altered from greenish blue to intense reddish purple (Figure 45). Figure 45 to Figure 52 detail the stone and the changes that were noted

following heating; Figure 46, Figure 47, and Figure 48 show a clear change in the color from yellow to reddish brown of material lining channels and some fractures and clearer indications of color bleeding into the tourmaline than were noted in stones heated for only 10 hours. Figure 49 to Figure 51 again detail a significant change in color appearance of both channels and fractures (the right hand images of Figure 51 also showing indications of color bleeding into the host tourmaline) while Figure 52 shows the cross-section of the broken end of the stone (broken during the heating process, see Figure 45) at two magnifications detailing the extent to which the material lining channels and fractures becomes mobile during the heating process and both changes color and lines all available fractures.

For stone 0668227702 before heating at 700°C the color of the sample was blue, after heating it changed to a reddish brown / blue mixture (Figure 54). Figure 55, Figure 56 and Figure 57 depict a single large fracture at differing angles and magnifications both before and after heating. The change in color appearance of the fracture is rather striking. The lower portion of the right hand image in Figure 56 also shows several smaller fractures that are colored reddish brown following treatment. These smaller fractures are further depicted in Figure 61 and Figure 62 where possible bleeding of color into the host tourmaline maybe seen.

The color of sample 0668228002 before heating at 700°C was green, after treatment this changed to an intense purplish red (Figure 64). The change in the appearance of this stone is possibly one of the most striking. Figure 65, Figure 66 and Figure 67 reveal the intensity of the changes to specific areas of the stone. While Figure 68 shows how the reddish brown post heating color appears in multiple smaller fractures.

Stone 0668226602 before heating was greenish blue while after it had gained a slight purplish appearance - not as striking a change as previous stones in the group (Figure 70). However, one group of fine fractures (Figure 73 and Figure 74) shows how in this instance the material (and therefore the color) is lining the surfaces of the fracture with the color apparently showing some slight bleeding into the stone.

To some extent the forgoing has also been noted by GIT researchers (GIT, 2009) who have carried out similar experiments. Our observations are still being assessed in the wider context of the experiments but it is curious to note the similarities in color between the phenomena described in Annex A from page 35 and the colors produced within channels and fractures after heating. Further, we need to collect optical data on the treated stones and then make thin-sections from several of the stones in this group to establish whether the color 'bleeding' is an optical effect, the result of diffusion, or a combination of both.



Figure 9: Sample 0668225902 before heating

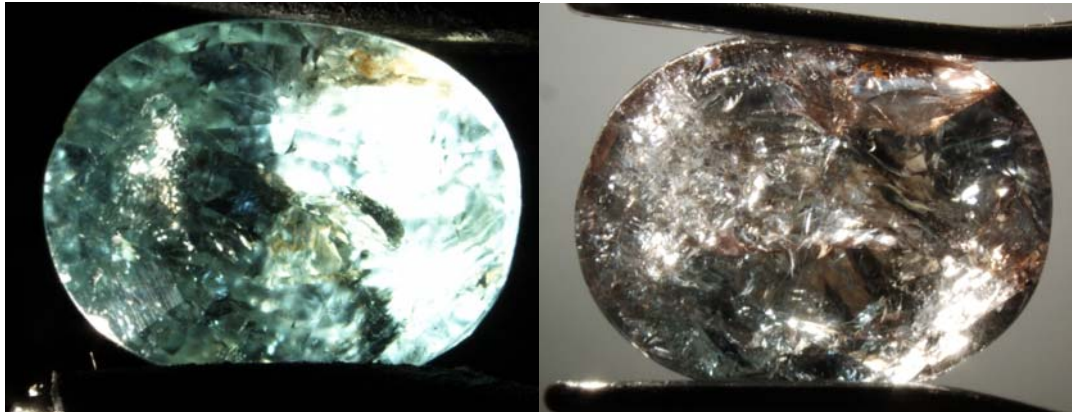


Figure 10: Sample 0668225902 before (left) after heating at 700°C in air **for 10 hours** (right); no foreign elements were added before or during the heating process. The overall face-up color impression changes from greenish blue to slightly purplish.



Figure 11: Sample 0668225902 comparable areas before (left) after heating at 700°C in air **for 10 hours** (right); no foreign elements were added before or during the heating process.



Figure 12: Sample 0668227002 before heating



Figure 13: Sample 0668227002 before (left) after heating at 700°C in air **for 10 hours** (right); no foreign elements were added before or during the heating process. The overall face-up color impression changes from green to slightly purplish.



Figure 14: Sample 0668227002 comparable areas before (left) after heating at 700°C in air **for 10 hours** (right); no foreign elements were added before or during the heating process (see Figure 15 for a closer study).

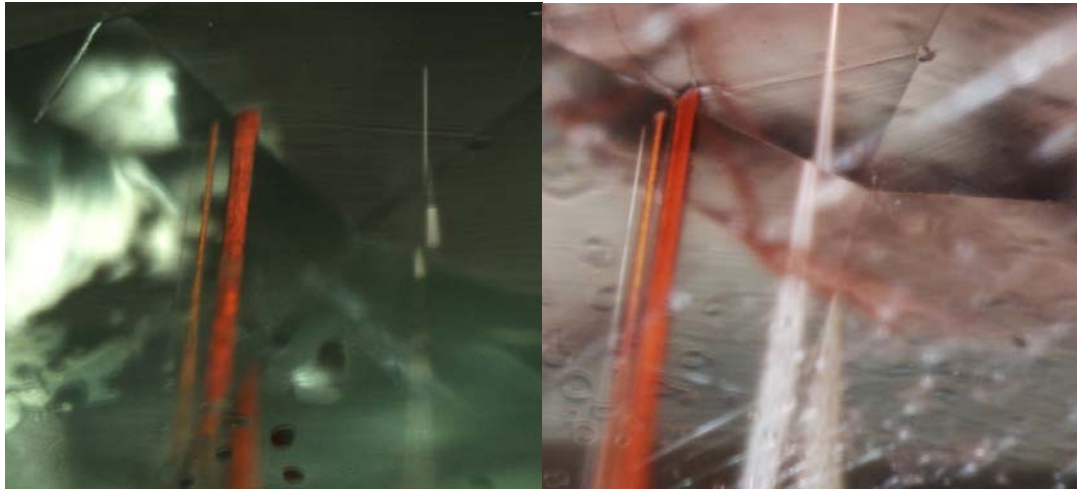


Figure 15: Sample 0668227002 comparable areas before (left) after heating at 700°C in air for 10 hours (right); no foreign elements were added before or during the heating process. In the right-hand image it can be seen that the color within the channel is more even and is slightly more towards orange; also a purplish-pink color has appeared within a fracture to the right of the channel.



Figure 16: Sample 0668227002 comparable areas before (left) after heating at 700°C in air for 10 hours (right); no foreign elements were added before or during the heating process. (see Figure 17 for a closer study).

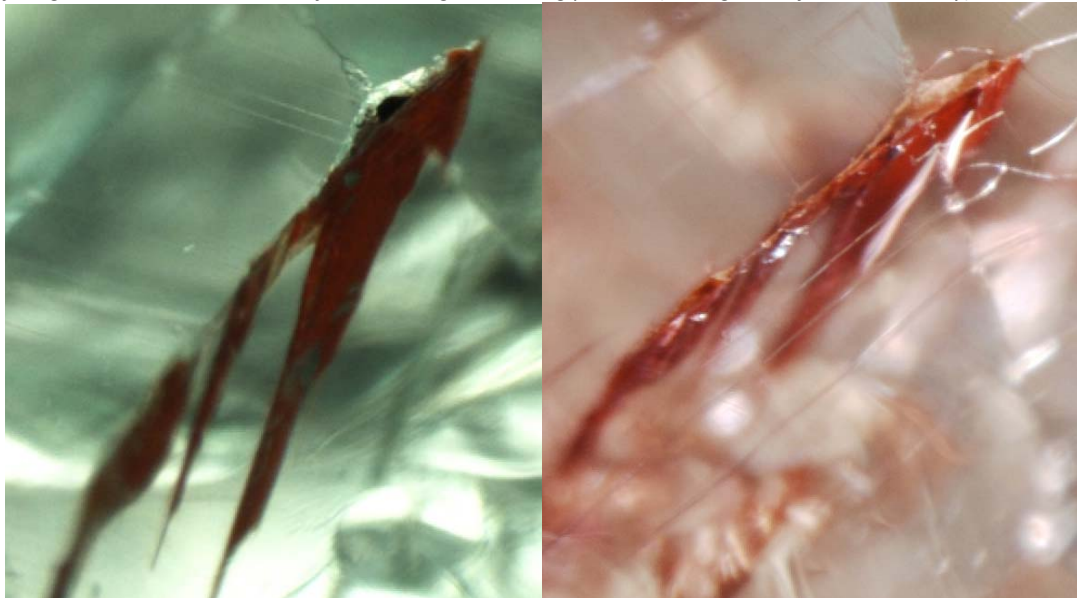


Figure 17: Sample 0668227002 comparable areas before (left) after heating at 700°C in air for 10 hours (right); no foreign elements were added before or during the heating process. The dark brown color of the material contained within the fracture in the left-hand image, has changed to brownish red in the right-hand image. This change has also impacted the background color. A close examination of the image on the right also indicates a possibility of the color 'bleeding' into the body of the stone from the fracture.

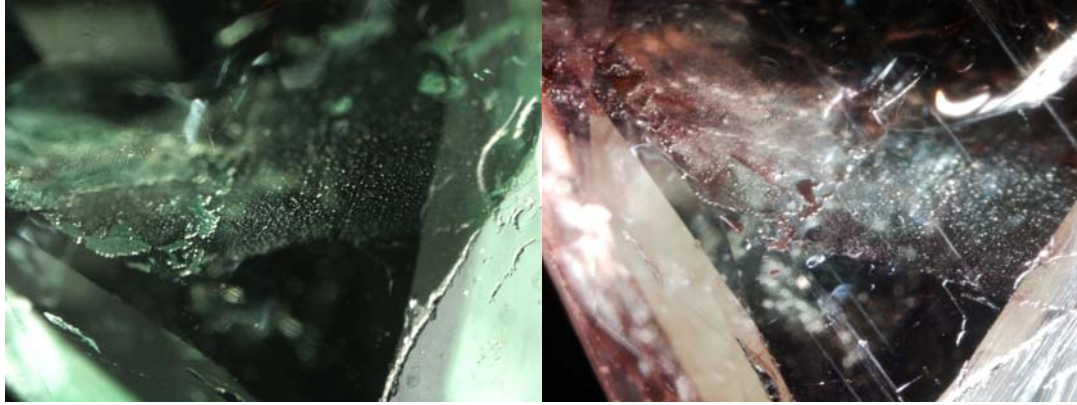


Figure 18: Sample 0668227002 comparable areas before (left) after heating at 700°C in air for 10 hours (right); no foreign elements were added before or during the heating process (see Figure 19 for a closer study).

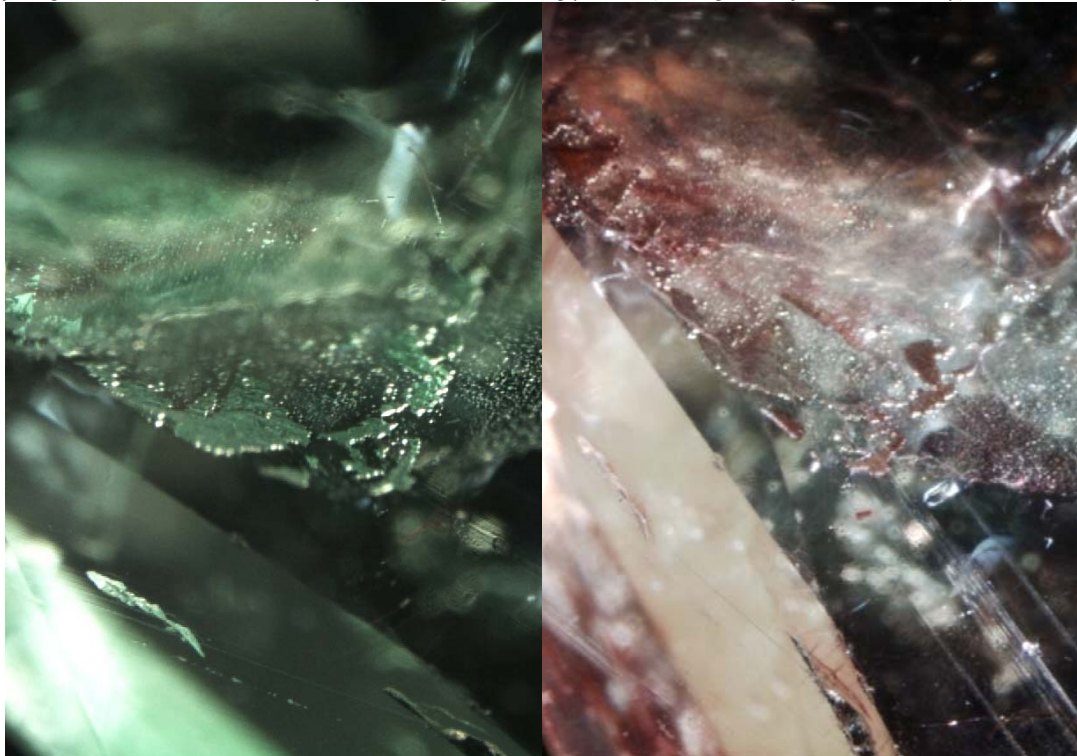


Figure 19 Sample 0668227002 comparable areas before (left) after heating at 700°C in air for 10 hours (right); no foreign elements were added before or during the heating process. It would appear that the brown material with the fractures in this group of tourmalines not only changes color but also becomes quite mobile at 700°C in air. The fracture in the image on the left shows no indication of the brown material within; however, this same fracture appears brownish red after heating (right).



Figure 20: Sample 0668227202 before heating



Figure 21: Sample 0668227202 before (left) and after heating at 700°C in air **for 10 hours** (right); no foreign elements were added before or during the heating process. The overall color impression has changed following heating from bluish (left) to purplish (right)

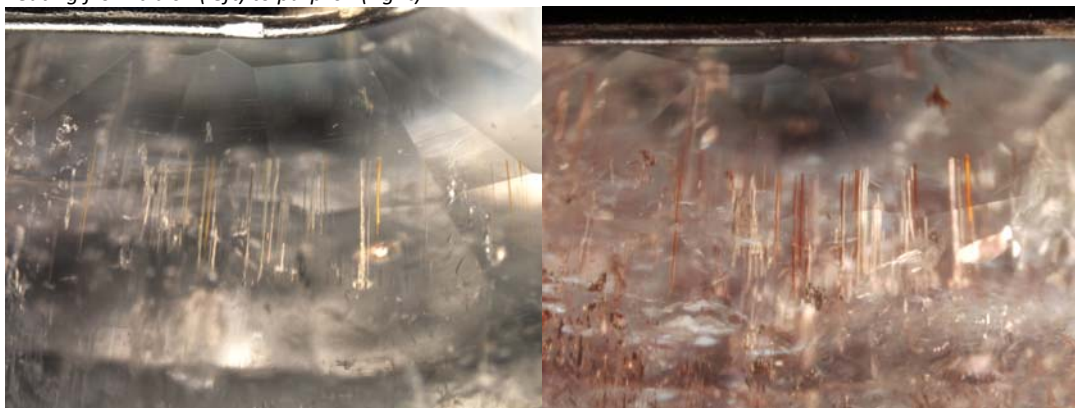
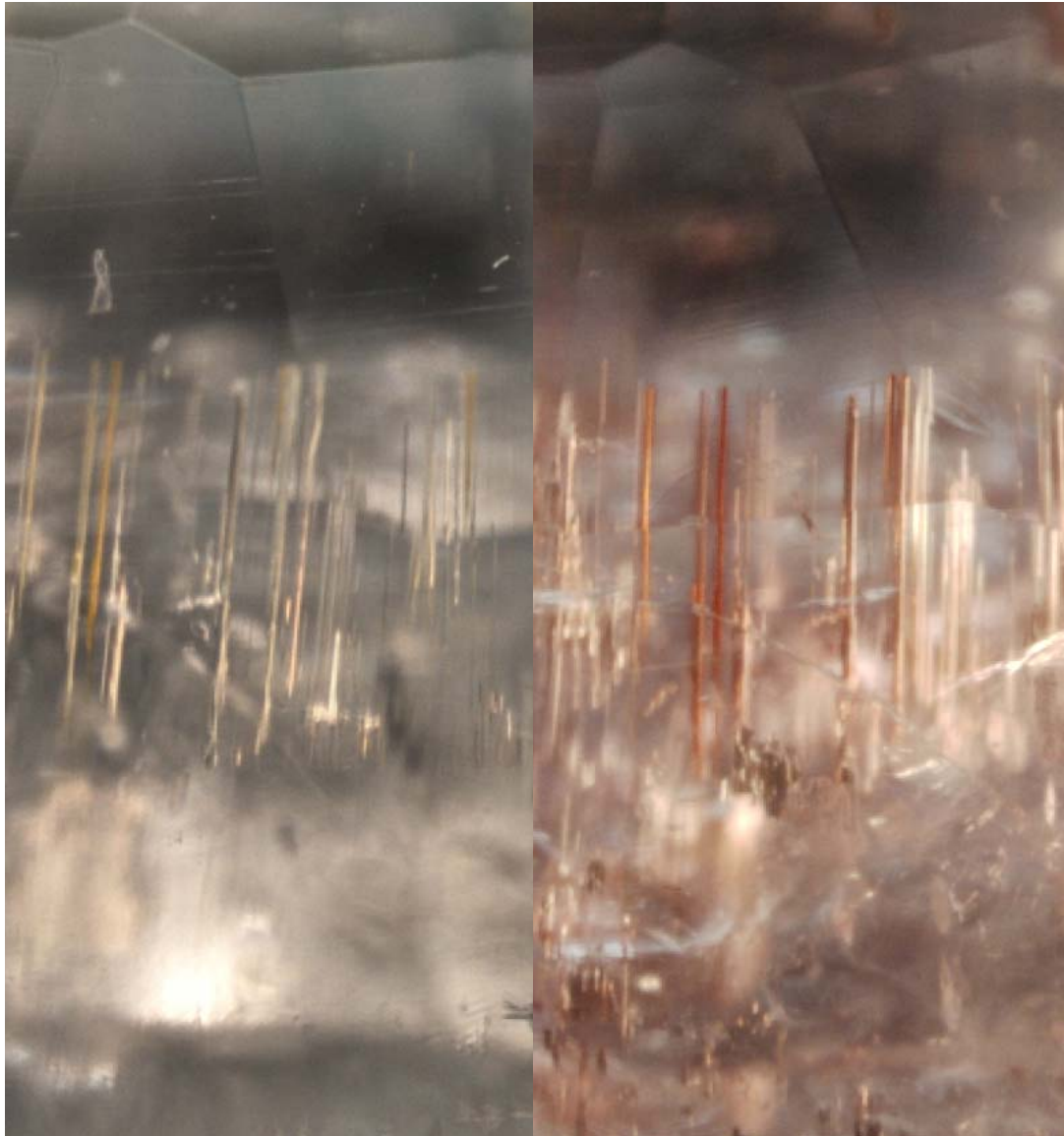


Figure 22: Sample 0668227202 comparable areas before (left) after heating at 700°C in air **for 10 hours** (right); no foreign elements were added before or during the heating process (see Figure 23 for a closer study).



*Figure 23: Sample 0668227202 comparable areas before (left) after heating at 700°C in air **for 10 hours** (right) no foreign elements were added before or during the heating process. The material contained within the channels in the left-hand image, has changed to brownish red in the right-hand image. This change has also impacted the background color. A close examination of the image on the right also indicates a possibility of the color 'bleeding' into the body of the stone from the fracture.*



*Figure 24: Sample 0668227202 comparable areas before (left) and after heating at 700°C in air **for 10 hours** (right) no foreign elements were added before or during the heating process (see Figure 25 for a closer study).*

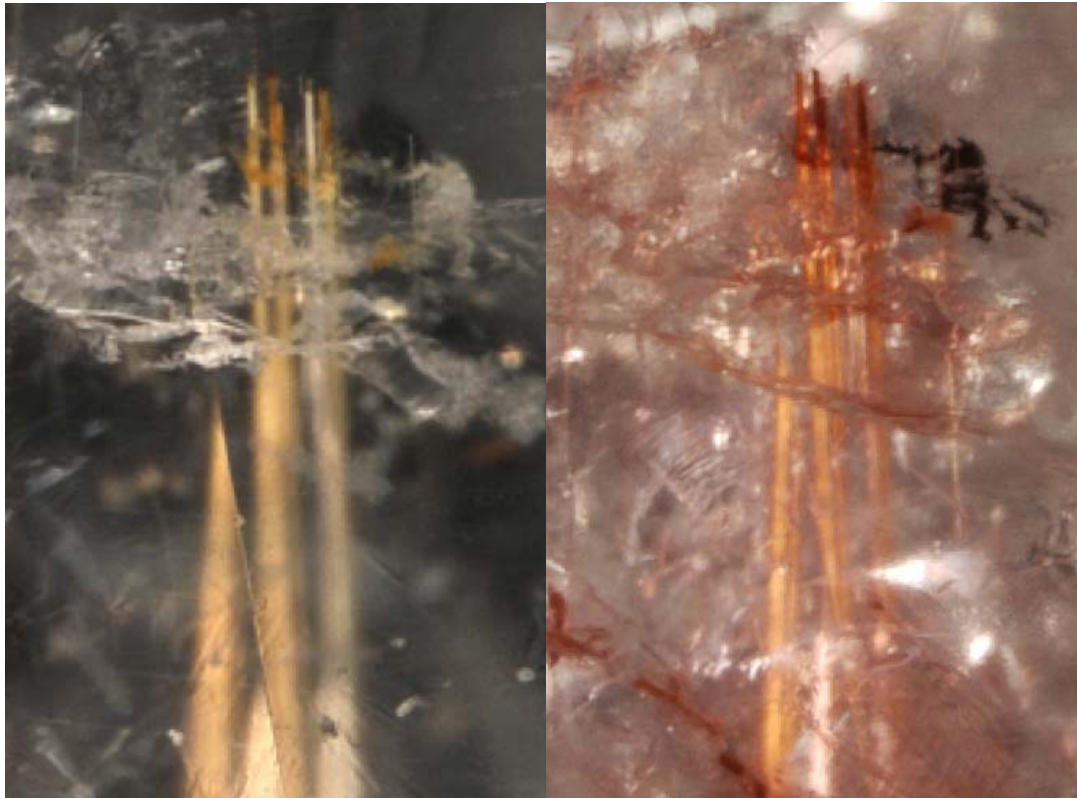


Figure 25: Sample 0668227202 comparable areas before (left) and after heating at 700°C in air for 10 hours (right) no foreign elements were added before or during the heating process. The yellow brown material held within the channels as seen in the left-hand images changes to reddish brown in the right-hand image. Further the material seems to have become mobile enough during the heating process to enter fractures and also change to reddish brown (right).



Figure 26: Sample 0668227202 comparable areas before (left) and after heating at 700°C in air for 10 hours (right) no foreign elements were added before or during the heating process (see Figure 27 for a closer study).

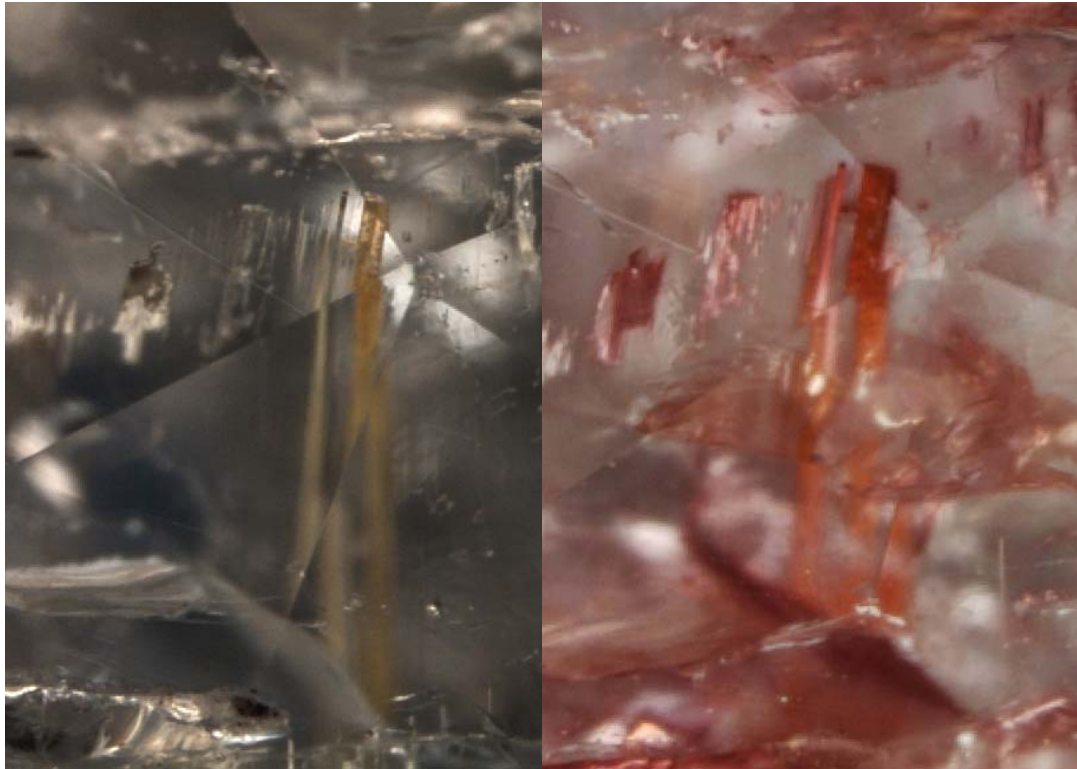


Figure 27: Sample 0668227202 comparable areas before (left) and after heating at 700°C in air for 10 hours (right) no foreign elements were added before or during the heating process. The material within the channels in the left-hand image changes from yellowish brown to brownish red following heat treatment (right). In addition fractures that previously did not appear to contain the yellowish brown material, appear reddish brown following heating (right).

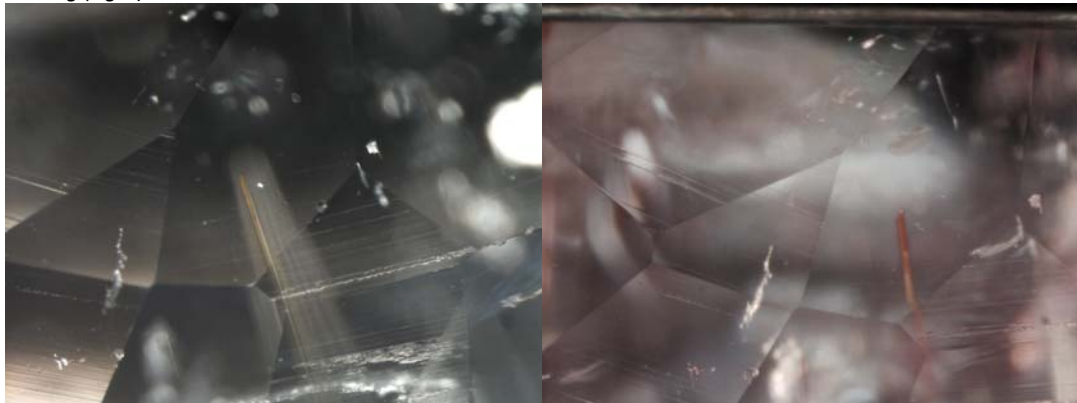


Figure 28: Sample 0668227202 comparable areas before (left) after heating at 700°C in air for 10 hours (right) no foreign elements were added before or during the heating process.



Figure 29: Sample 0668228402 before heating

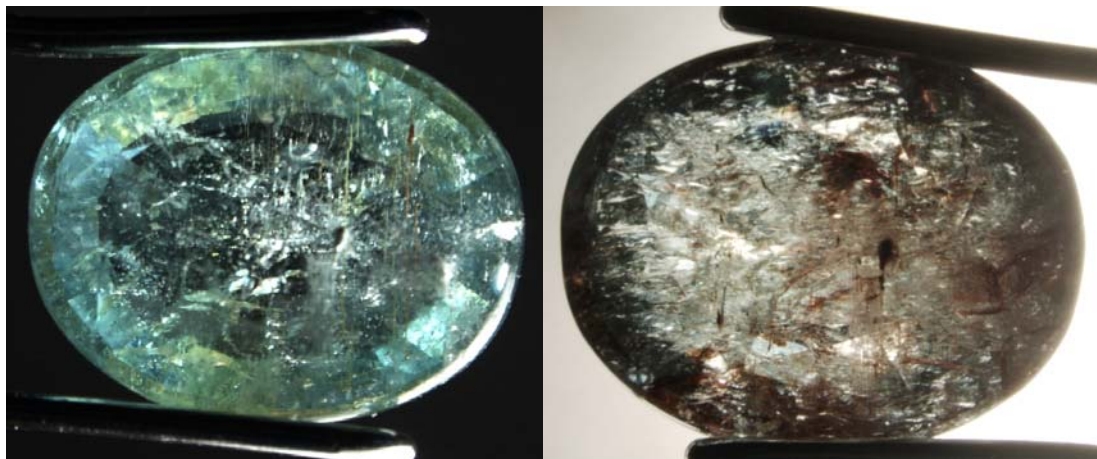


Figure 30: Sample 0668228402 before (left) and after heating at 700°C in air **for 10 hours** (right) no foreign elements were added before or during the heating process. The face-up color appearance changed from a greenish blue to a purplish appearance after heating.

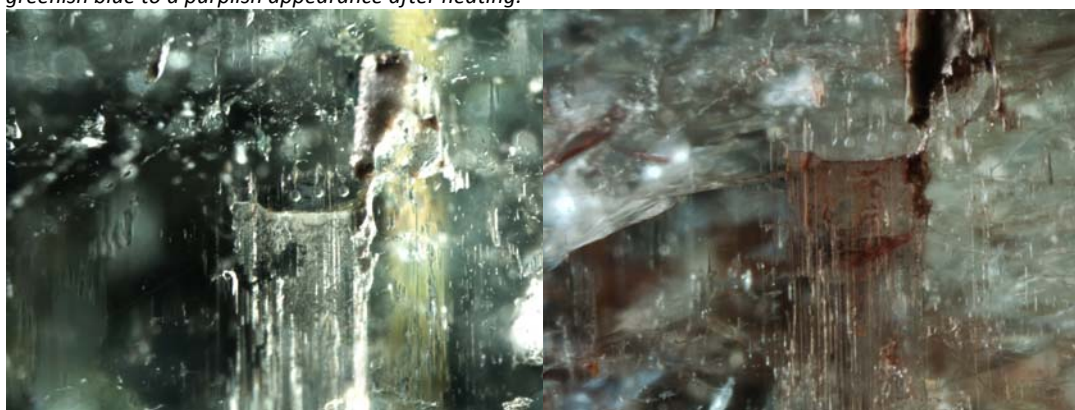


Figure 31: Sample 0668228402 comparable areas before (left) after heating at 700°C in air **for 10 hours** (right) no foreign elements were added before or during the heating process (see Figure 32 for a closer study).



Figure 32: Sample 0668228402 comparable areas before (left) after heating at 700°C in air **for 10 hours** (right); no foreign elements were added before or during the heating process. The inside of the fracture (left) became a reddish brown after heating (right).

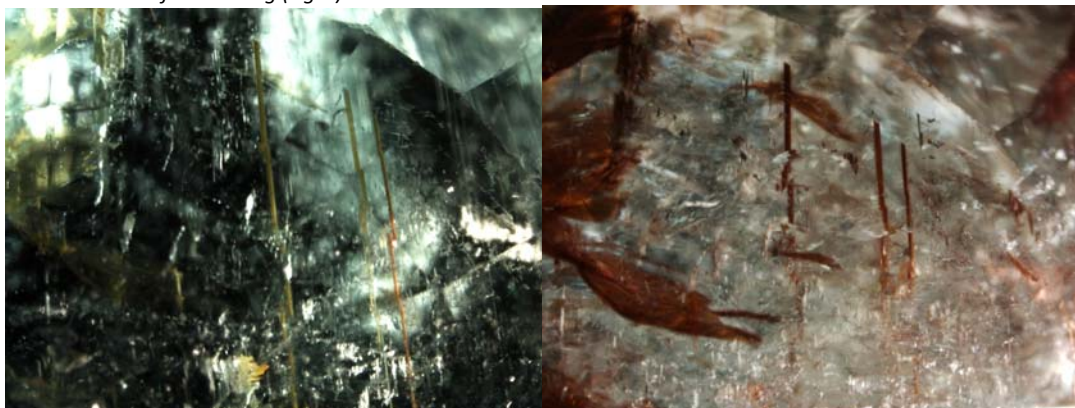


Figure 33: Sample 0668228402 comparable areas before (left) after heating at 700°C in air **for 10 hours** (right); no foreign elements were added before or during the heating process. The yellowish material filling the channels running north-south (left) became deep reddish brown following heating (right) along with the fracture lower left (right).



Figure 34: Sample 0668228402 comparable areas before (left) and after heating at 700°C in air for 10 hours (right); no foreign elements were added before or during the heating process. Here a fracture with a small amount of dark material present prior to heating has become a deep reddish brown throughout. Several channels have also become a reddish brown. These changes have also impacted the general color appearance of the area following the heat treatment.



Figure 35: Sample 0668228402 comparable areas before (left) and after heating at 700°C in air for 10 hours (right); no foreign elements were added before or during the heating process. The color of these channels running top left to bottom right has changed from yellowish before heat treatment (left) to a deep reddish brown after (right). A fracture associated with the channel on the right also became reddish brown after heating.

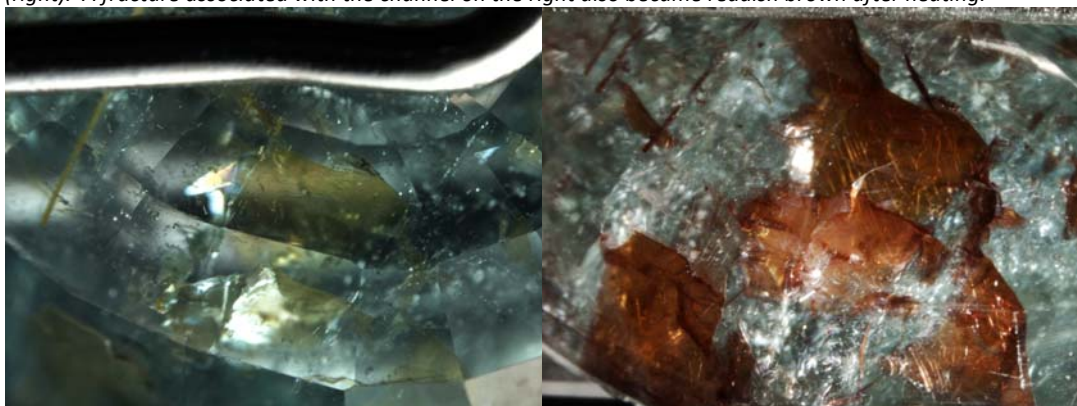


Figure 36: Sample 0668228402 comparable areas before (left) and after heating at 700°C in air for 10 hours (right); no foreign elements were added before or during the heating process. A fracture containing a light brownish material before heating (left) became a deep reddish brown after heating (right).

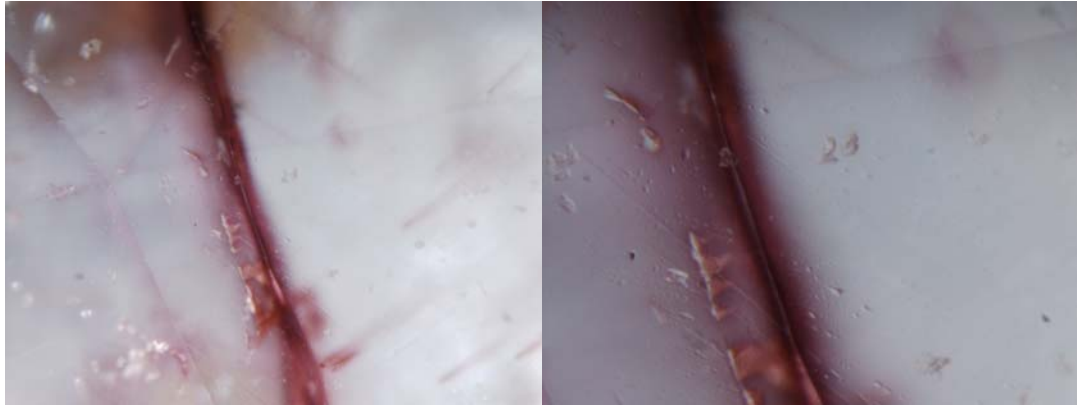


Figure 37: A fracture in sample 0668227202 after heating at 700°C in air for 10 hours (left) and the same area at a higher magnification (right); no foreign elements were added before or during the heating process. Here the material within is shown to be lining the walls of the fracture and in addition there is a distinct impression that the color is bleeding into the body of the tourmaline.



Figure 38: Channels in sample 0668227202 after heating at 700°C in air for 10 hours. In these images, similarly to that seen in Figure 37, there is a distinct impression that the color in these channels is bleeding into the body of the tourmaline.



Figure 39: Channels in sample 0668227202 after heating at 700°C in air for 10 hours. In these images, similarly to that seen in Figure 37 and Figure 38, there is a distinct impression that the color in these channels is bleeding into the body of the tourmaline.



Figure 40: Channels in samples 0668228402 (left) 0668227202 (right) after heating at 700°C in air for 10 hours. In these images, similarly to that seen in Figure 37, Figure 38 and Figure 39, there is a distinct impression that the color in these channels is bleeding into the body of the tourmaline.

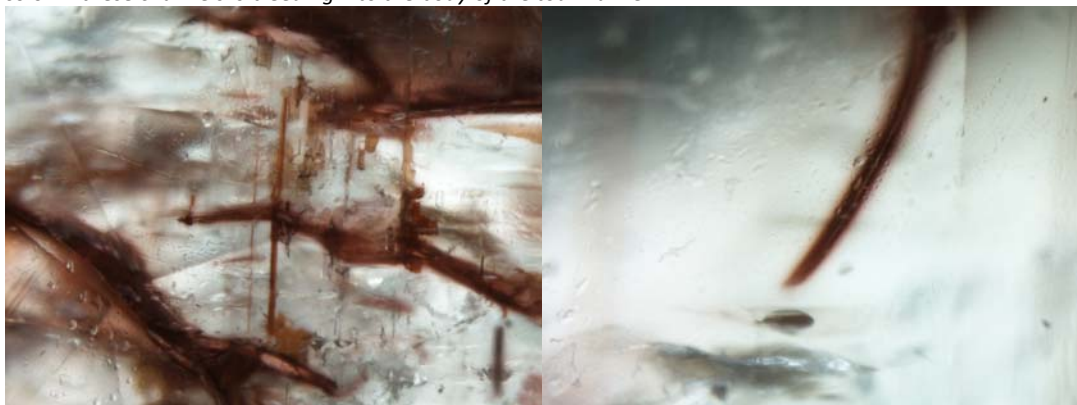


Figure 41: Fractures in sample 0668228402 after heating at 700°C in air for 10 hours. There is a distinct impression that the color within these fractures is bleeding into the body of the tourmaline.

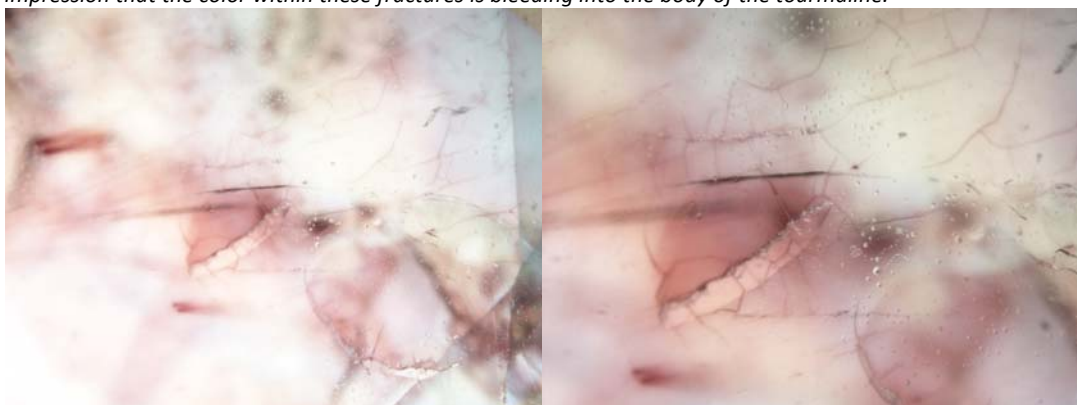


Figure 42: Fine fractures in sample 0668228402 after heating at 700°C in air for 10 hours (left) and at higher magnification (right) and in Figure 43.



Figure 43: Fine fractures in sample 0668228402 after heating at 700°C in air **for 10 hours** (left) and at higher magnification (right). See also Figure 42.



Figure 44: 0668227502 before heating

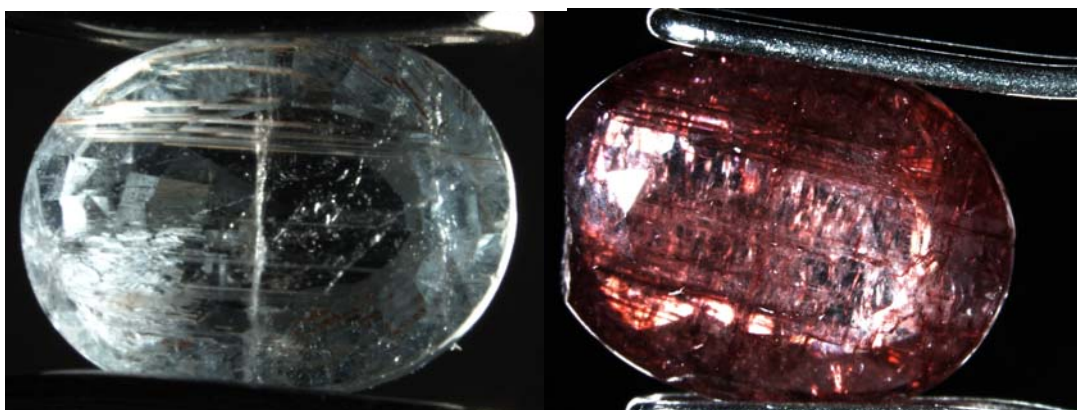


Figure 45: 0668227502 before heating (left) and after heating at 700°C in air **for 100 hours**; no foreign elements were added before or during the heating process. Here the face-up color appearance has considerably altered from greenish blue to an intense reddish purple. Note that the left portions of this stone broke off during the heating process, see Figure 52 for detail.

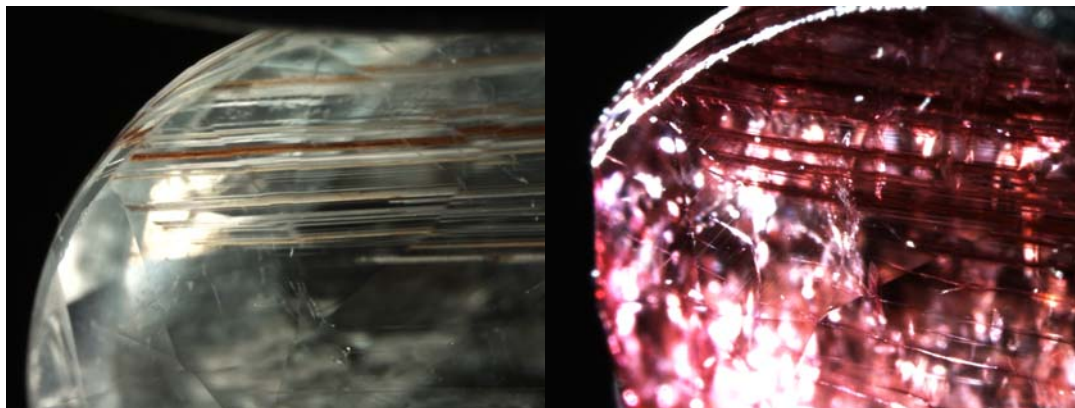


Figure 46: 0668227502 comparable areas before heating (left) and after heating at 700°C in air for 100 hours; no foreign elements were added before or during the heating process. The brown material within the channels running left to right in the upper portion of this figure have changed from brown (left) to reddish purple (right) and the color appears to bleed into the tourmaline(right).

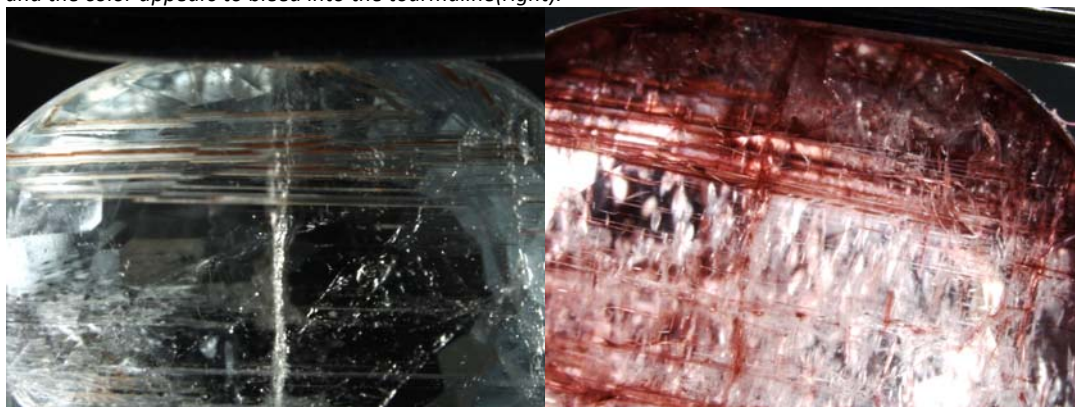


Figure 47: 0668227502 comparable areas before heating (left) and after heating at 700°C in air for 100 hours; no foreign elements were added before or during the heating process. A wider view of that seen in Figure 46 and showing similar effect in the channels plus within some fractures.

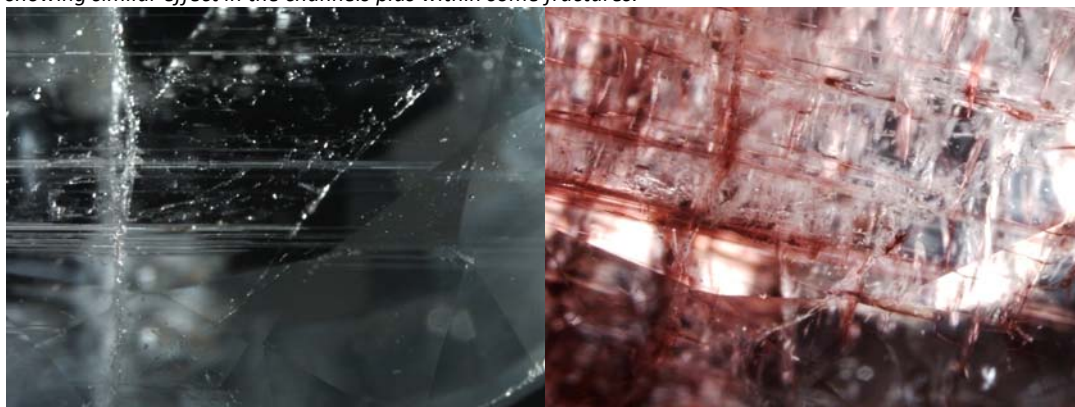


Figure 48: 0668227502 comparable areas before heating (left) and after heating at 700°C in air for 100 hours; no foreign elements were added before or during the heating process. This figure details the lower portion of Figure 47 and the before and after appearance of fractures within that area. Again, there appears to be some color bleeding into the tourmaline from the fractures.

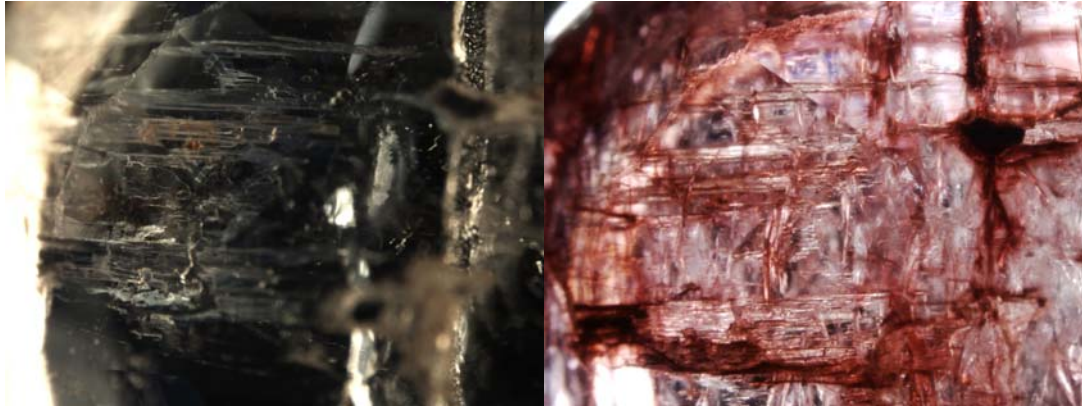


Figure 49: 0668227502 comparable areas before heating (left) and after heating at 700°C in air for 100 hours; no foreign elements were added before or during the heating process. The color of the material within fractures appears to have changed from yellowish to an intense reddish brown.

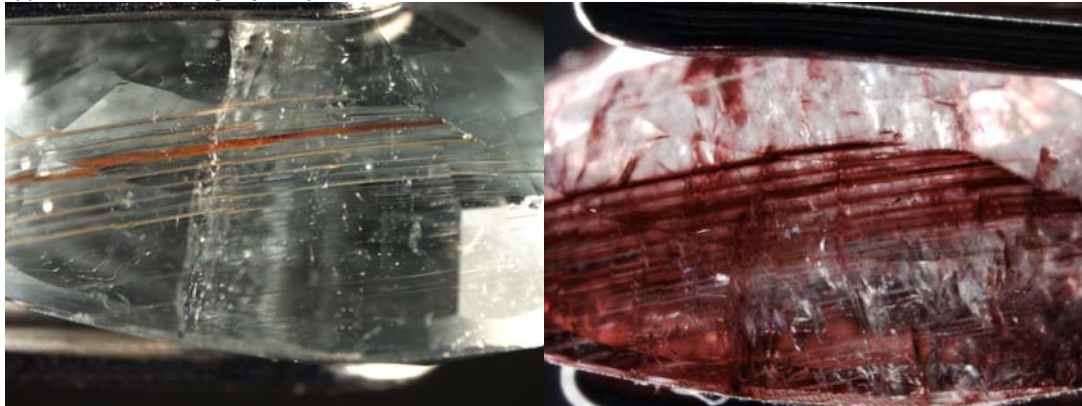


Figure 50: 0668227502 comparable areas before heating (left) and after heating at 700°C in air for 100 hours; no foreign elements were added before or during the heating process. The color of the material within the channels running left to right appear to have changed from yellowish brown to an intense reddish brown.

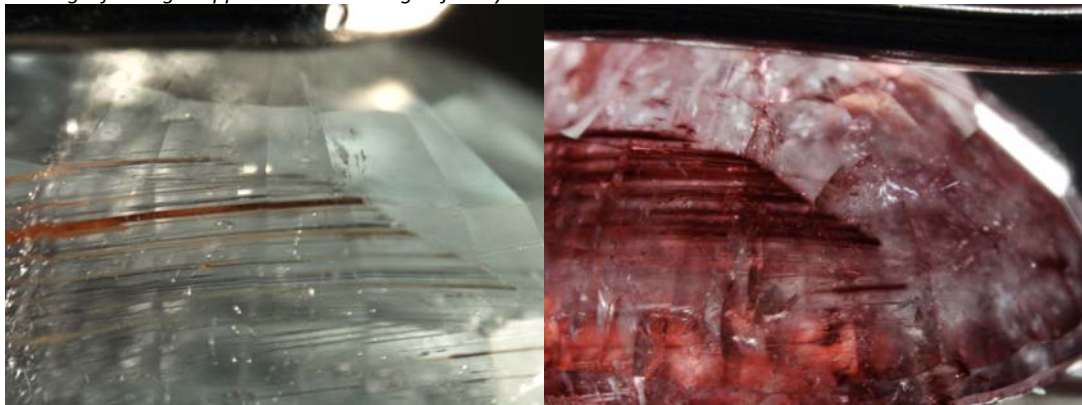


Figure 51: 0668227502 comparable areas before heating (left) and after heating at 700°C in air for 100 hours; no foreign elements were added before or during the heating process. The color of the material within the channels running left to right appear to have changed from yellowish brown to an intense reddish brown and fractures surrounding these have gained the same color.

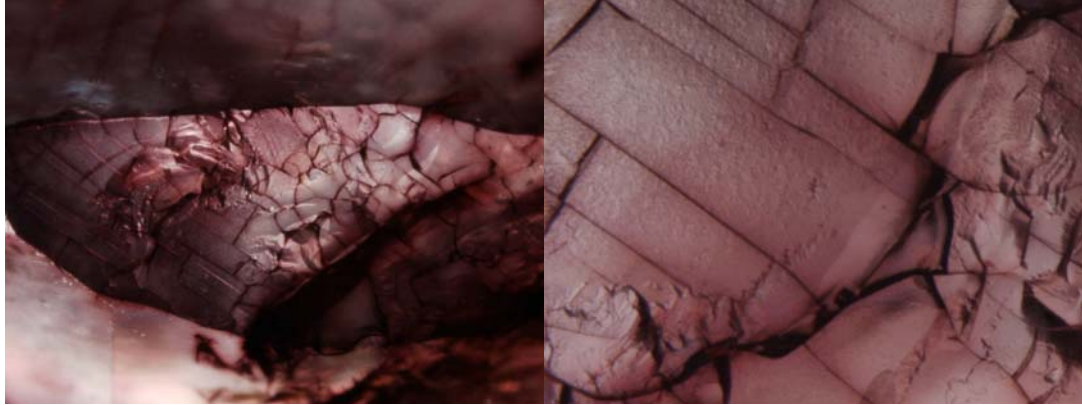


Figure 52: 0668227502 after heating at 700°C in air for 100 hours; no foreign elements were added before or during the heating process. This figure shows detail of the broken end of this stone and the penetration of the material now within the fractures.



Figure 53: 0668227702 before heating

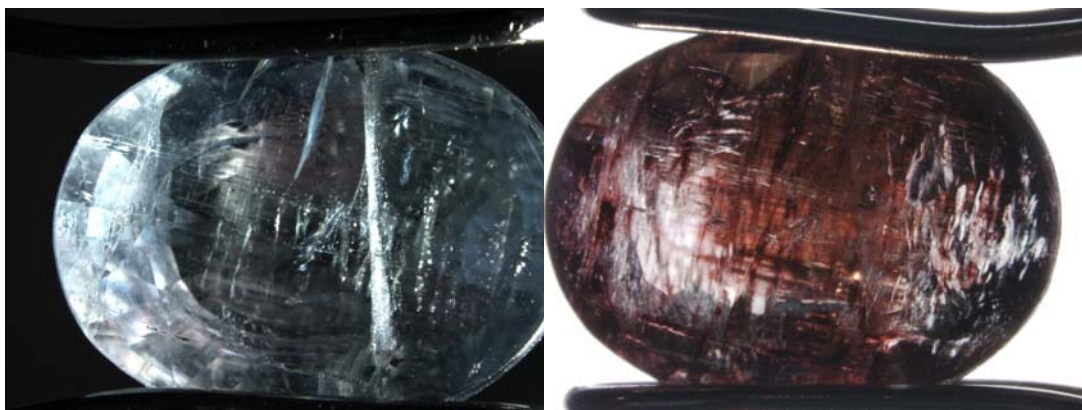


Figure 54: 0668227702 before heating (left) and after heating at 700°C in air for 100 hours; no foreign elements were added before or during the heating process. The apparent color of the sample changed from blue to a mixture of reddish brown and blue after heating.

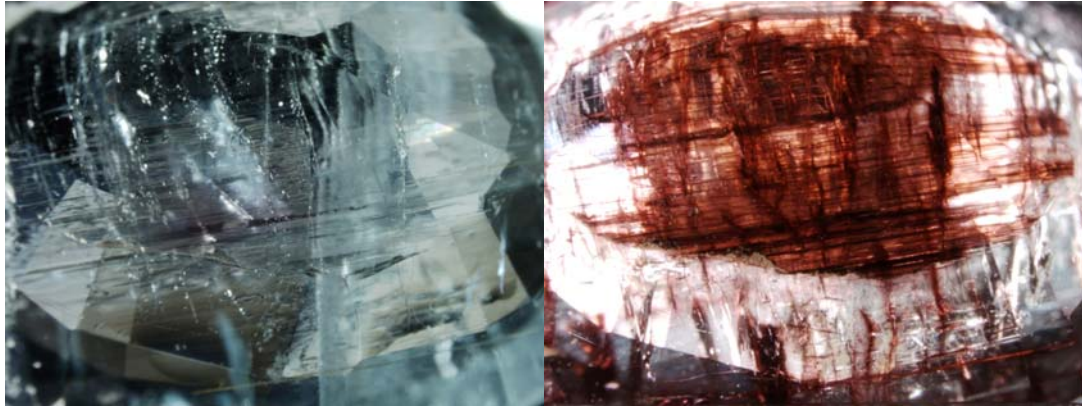


Figure 55: 0668227702 comparable areas before heating (left) and after heating at 700°C in air **for 100 hours**; no foreign elements were added before or during the heating process. A large plus numerous smaller fractures appear reddish brown following the heat treatment process, see also Figure 56.

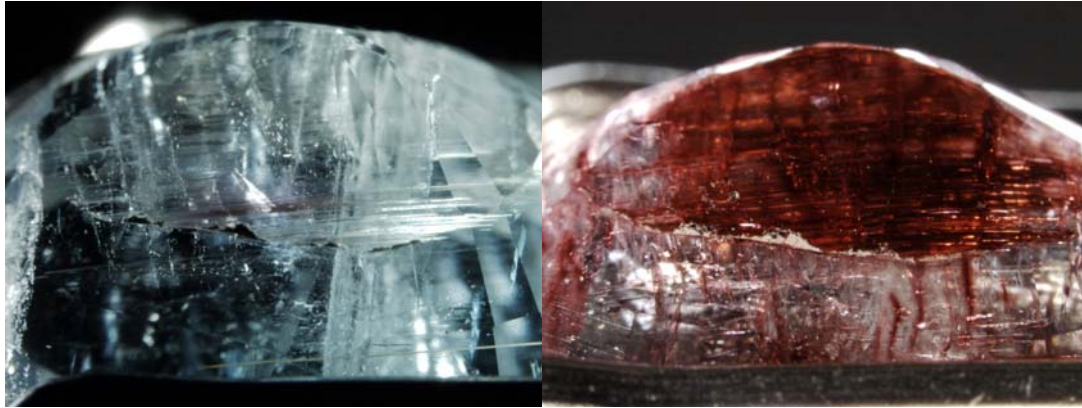


Figure 56: 0668227702 comparable areas before heating (left) and after heating at 700°C in air **for 100 hours**; no foreign elements were added before or during the heating process. A view of the fracture seen in Figure 55 from a different (lower) angle, a dark material is apparent where the fracture meets the surface of the stone but is not seen deep within prior to heating (left) after heating the fracture appears a distinct reddish brown.

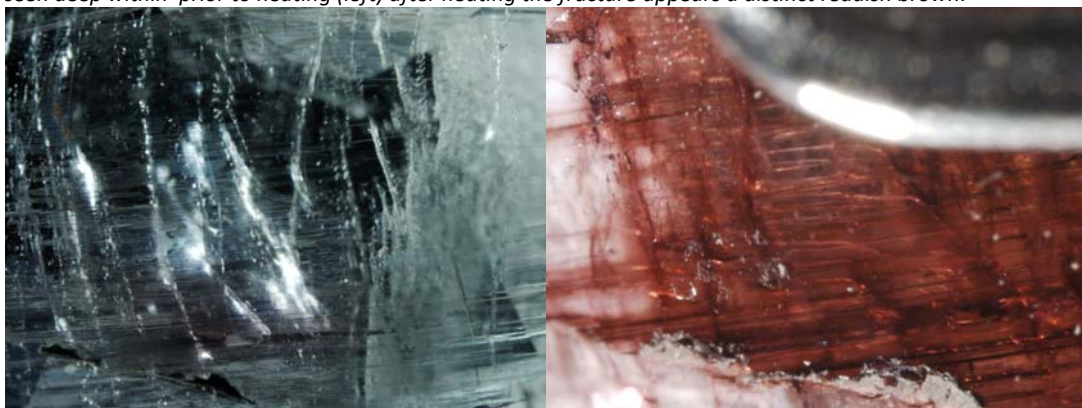


Figure 57: 0668227702 comparable areas before heating (left) and after heating at 700°C in air **for 100 hours**; no foreign elements were added before or during the heating process. A closer view of the fracture seen in Figure 55 and Figure 56 showing the dark material that is apparent where the fracture meets the surface of the stone but is not seen deep within prior to heating (left) after heating the fracture appears a distinct reddish brown while the material present where the fracture meets the surface now appears light in color..



Figure 58: 0668227702 comparable areas before heating (left) and after heating at 700°C in air **for 100 hours**; no foreign elements were added before or during the heating process. The partially visible fracture in the center of the image on the left appears reddish brown in the image on the right.



Figure 59: 0668227702 comparable areas before heating (left) and after heating at 700°C in air **for 100 hours**; no foreign elements were added before or during the heating process. The partially visible fracture in the left-center of the image on the left appears reddish brown in the image on the right as do several other fractures following the heat treatment process.



Figure 60: 0668227702 comparable areas before heating (left) and after heating at 700°C in air **for 100 hours**; no foreign elements were added before or during the heating process. The partially visible fracture in the center of the image on the left and the fracture running west-east at the bottom of the image appear reddish brown in the image on the right as do several other fractures following the heat treatment process.

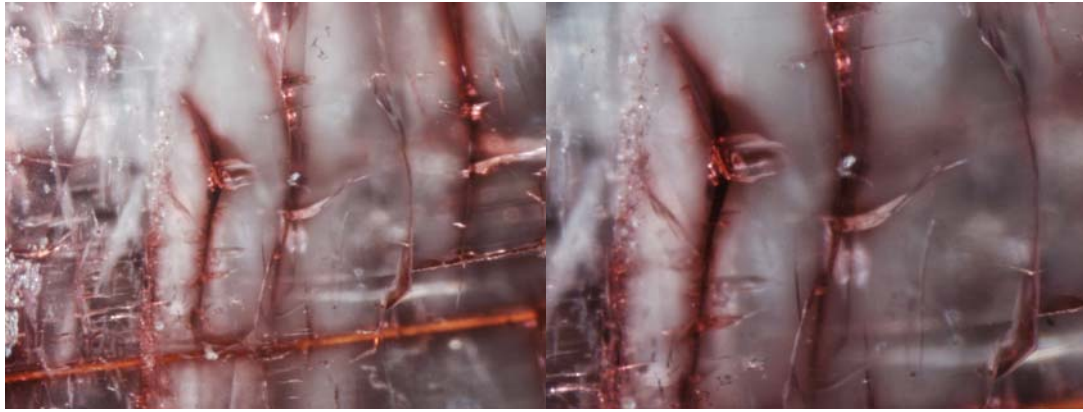


Figure 61: 0668227702 after heating at 700°C in air for 100 hours; no foreign elements were added before or during the heating process. Deep reddish brown coloration in fractures running north-south (left) with a higher magnification (right), color appears to bleed into the tourmaline host.



Figure 62: 0668227702 after heating at 700°C in air for 100 hours; no foreign elements were added before or during the heating process. A higher magnification of the fracture seen in Figure 61 (right). The deep reddish brown coloration appears to bleed into the tourmaline host.



Figure 63: 0668228002 before heating



Figure 64: 0668228002 before heating (left) and after heating at 700°C in air for 100 hours; no foreign elements were added before or during the heating process. The color appearance changed from green before treatment to an intense purplish red after treatment.

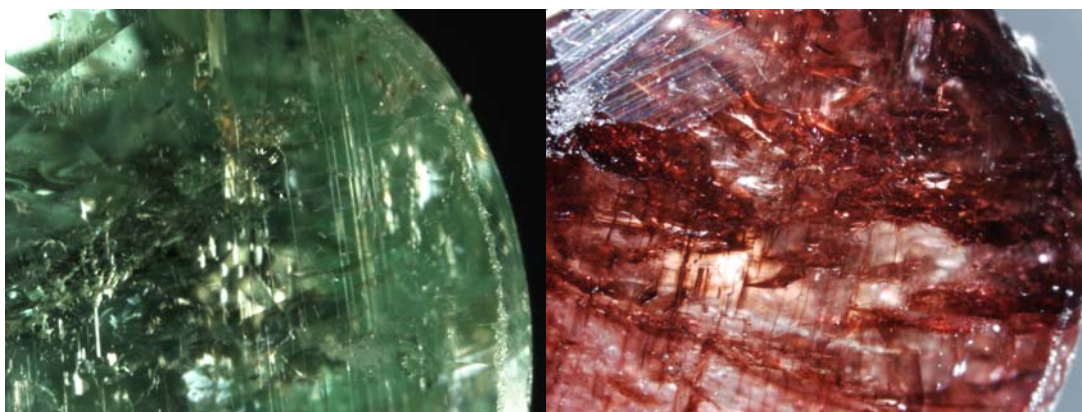


Figure 65: 0668228002 comparable areas before heating (left) and after heating at 700°C in air for 100 hours; no foreign elements were added before or during the heating process. The brownish material within fractures (left side of the left image) became an intense reddish brown after treatment (right).

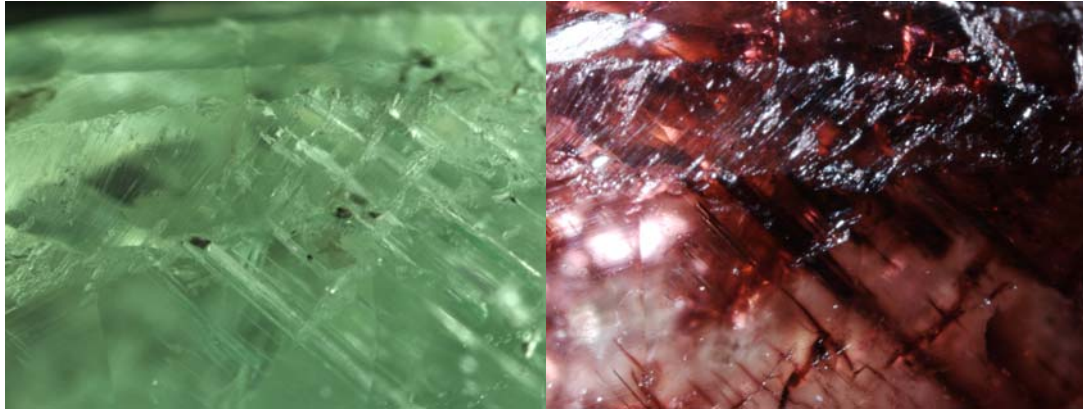


Figure 66: 0668228002 comparable areas before heating (left) and after heating at 700°C in air **for 100 hours**; no foreign elements were added before or during the heating process. A dark material can be seen at the entrance to the channels in the left-hand image which after heating (right) have become an intense reddish brown.

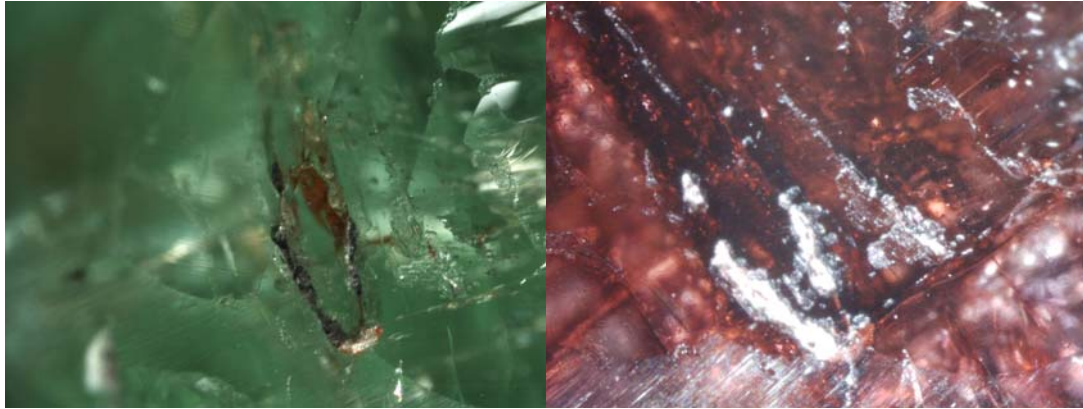


Figure 67: 0668228002 comparable areas before heating (left) and after heating at 700°C in air **for 100 hours**; no foreign elements were added before or during the heating process. Dark material seen in the centrally located fracture in the left-hand image has spread and become an intense reddish brown in the right-hand image.



Figure 68: 0668228002 after heating at 700°C in air **for 100 hours**; no foreign elements were added before or during the heating process. Numerous fractures now appear to be an intense brownish red.



Figure 69: 0668226602 before heating



Figure 70: 0668226602 before heating (left) and after heating at 700°C in air **for 100 hours**; no foreign elements were added before or during the heating process. Greenish blue before treatment, this stone now has a slight purplish appearance - not as striking a change as previous stones in the group.



Figure 71: 0668226602 comparable areas before heating (left) and after heating at 700°C in air **for 100 hours**; no foreign elements were added before or during the heating process. A slight purplish color has appeared in the fracture center top of the right-hand image after heating that was not present before.

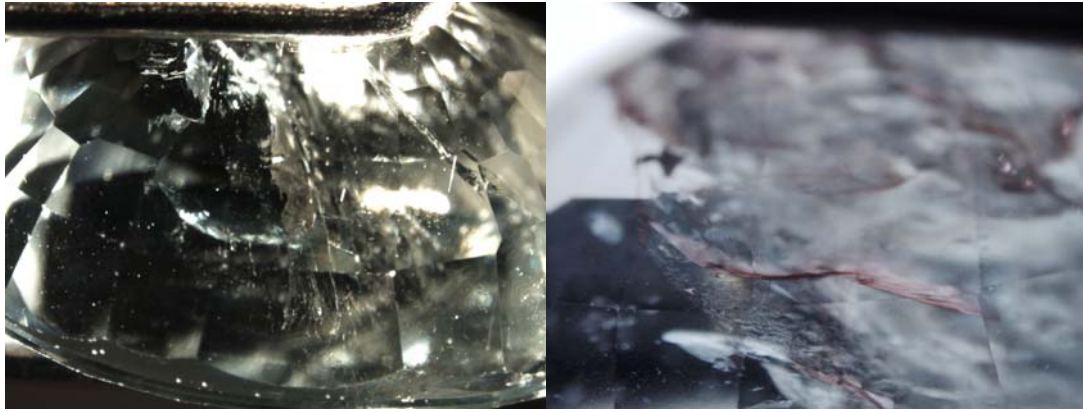


Figure 72: 0668226602 comparable areas before heating (left) and after heating at 700°C in air for 100 hours; no foreign elements were added before or during the heating process. A purplish color has appeared in the fracture center of the right-hand image after heating that was not present before (left).



Figure 73: 0668226602 after heating at 700°C in air for 100 hours; no foreign elements were added before or during the heating process. A purple color is seen to have appeared within several fractures. See Figure 74 for a closer view of the fracture seen lower right in the right hand image.



Figure 74: 0668226602 a closer view of the fracture seen lower right in the right-hand image in Figure 73. The purple color is appears to be strongest on the walls of the fracture and then fades into the tourmaline host.

Annex A:



Figure 75 Blue-green copper-bearing tourmaline (polished surface at center revealing the fracture related pinkish purple coloration), weighing 59.979 cts. Photo by Adirote Sripradi.

It has been suggested that the pinkish purple coloration surrounding surface reaching growth tubes and fractures in known natural untreated tourmaline is caused by natural radioactive fluids penetrating the stone (Koivula J. I., 2009, Koivula, 2009). Further, in the latest GRS journal (Peretti, 2009), the authors supported this assumption and deduced that the purple “halos” are indeed most likely induced by irradiation after detecting the presence of trace concentrations of the elements uranium and thorium within in the related cracks and tubes.

Following the lead of Koivula and Peretti et.al, GIA Laboratory, Bangkok, set about a process to confirm their results with further similar specimens. In particular a blue-green copper-bearing tourmaline with pinkish purple zones associated with growth tubes and fractures was obtained (Figure 75) from Richard Hughes (Senior Vice-President, Gemstone Marketing and Testing for NCS Group Co. Ltd.) In this study, the chemistry of the tourmaline sample was examined in detail to see if any radioactive elements such as uranium or thorium could be detected in the pinkish purple zones.

Raman spectroscopy was used (prior to any fabrication) to confirm that this stone was tourmaline. The inclusions present are the classic (tourmaline) trichites, partially healed fissures and growth tubes of which some are filled with a yellow material. Pinkish purple color zones are clearly evident and appear associated with some fractures and growth tubes. (See Figure 76 to Figure 79)



Figure 76: Partially healed fissures and growth tubes in the tourmaline examined for this study

Analysis of the rough surface

Prior to any fabrication, Laser ablation inductively coupled plasma mass spectrometry (LA-ICP-MS) was used to obtain a general chemical analysis of the stone and with this information establish that it was a Cu containing tourmaline as well as the most likely country of origin. The stone was found to contain 0.11 wt% CuO (847 ppmw of Cu; %RSD=12.24) and 2.25 wt% MnO (17434 ppmw of Mn; %RSD=6.66) establishing the type of tourmaline and following the use of a proprietary program, which compares several other trace elements, the country of origin was established as Mozambique (Abduriyim A., 2006).

Further, using LA- ICP-MS to map the chemistry of the rough surface a series of 24 samplings were taken of the stone from the green area right up to a fracture that contained a pinkish purple coloration (Figure 80). Neither thorium (^{232}Th) nor uranium (^{238}U) were detected in the green area however, both were detected in some pinkish purple colored areas (Figure 81 and Figure 82).



Figure 77: Yellow and red-brown hollow tubes breaking the surface of this tourmaline.



Figure 78: Unusual pinkish purple coloration in growth tubes and cracks in the sample stone.



Figure 79: An unusual pinkish purple cloud surrounding a growth tube in the tourmaline.

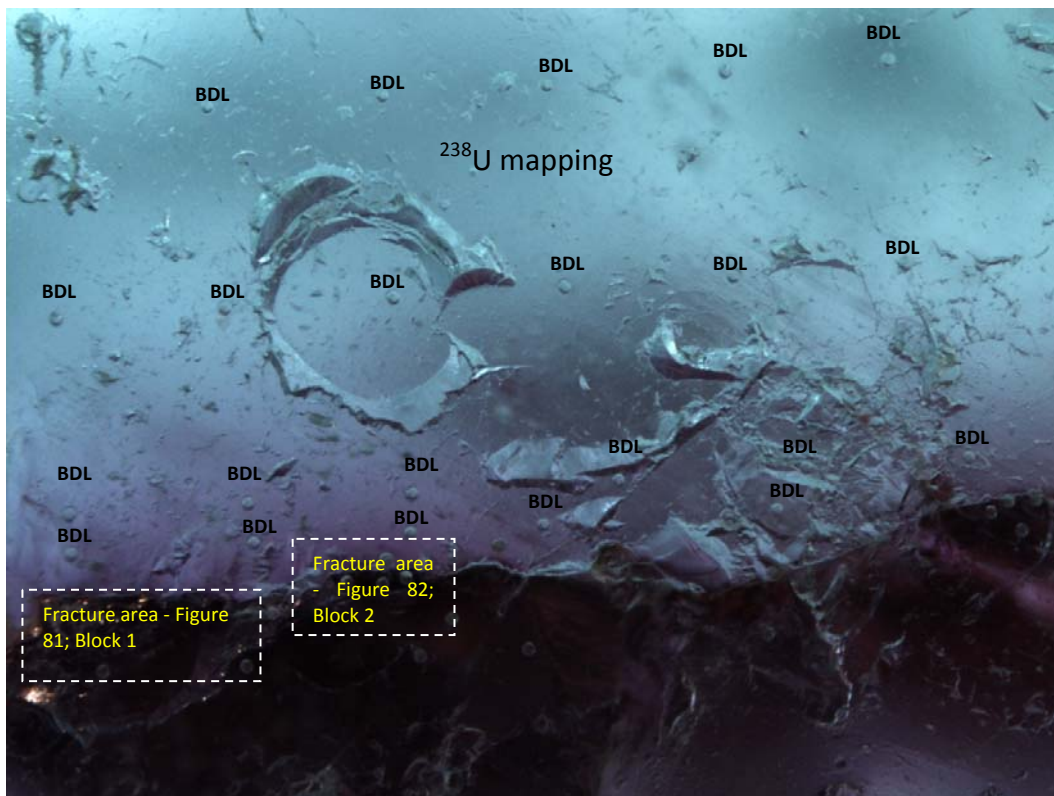


Figure 80: Photomicrograph of the ^{238}U mapping of the Mozambique tourmaline analyzed with by LA-ICP-MS (at the rough (un-ground) surface for this study). Each spot in the green area was below the detection limit (BDL) of the instrument for ^{238}U . The detection limit for ^{238}U was 0.01 ppmw).

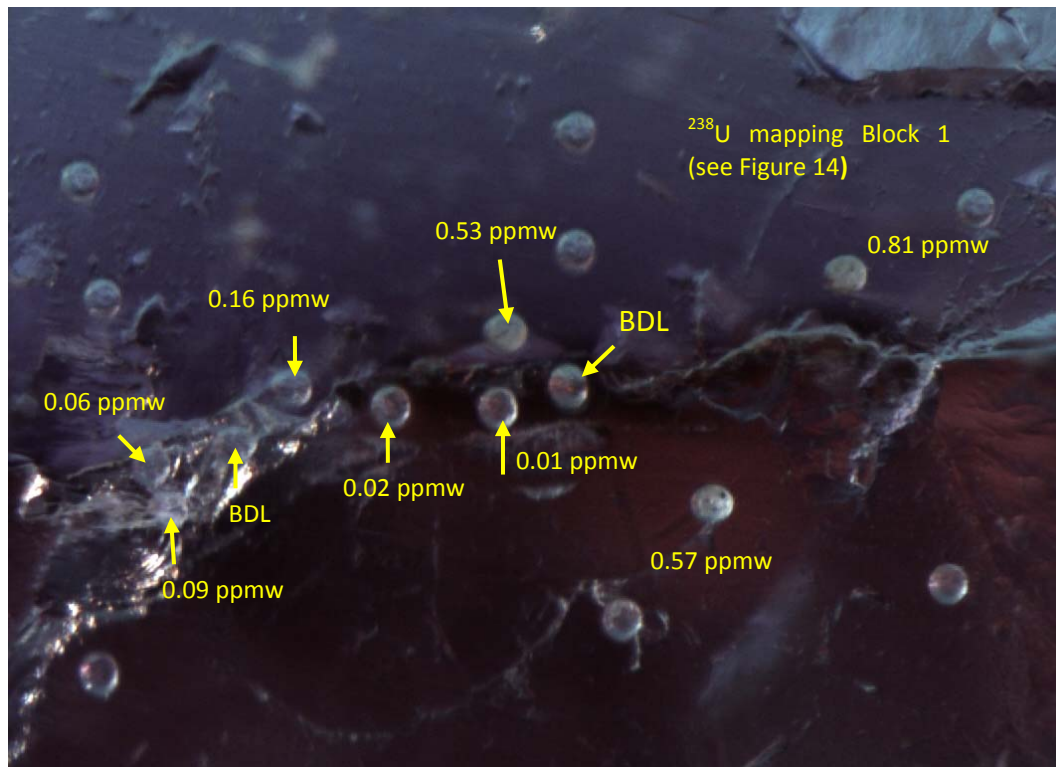


Figure 81: Enlarged photomicrograph of the ^{238}U mapping from Figure 80.

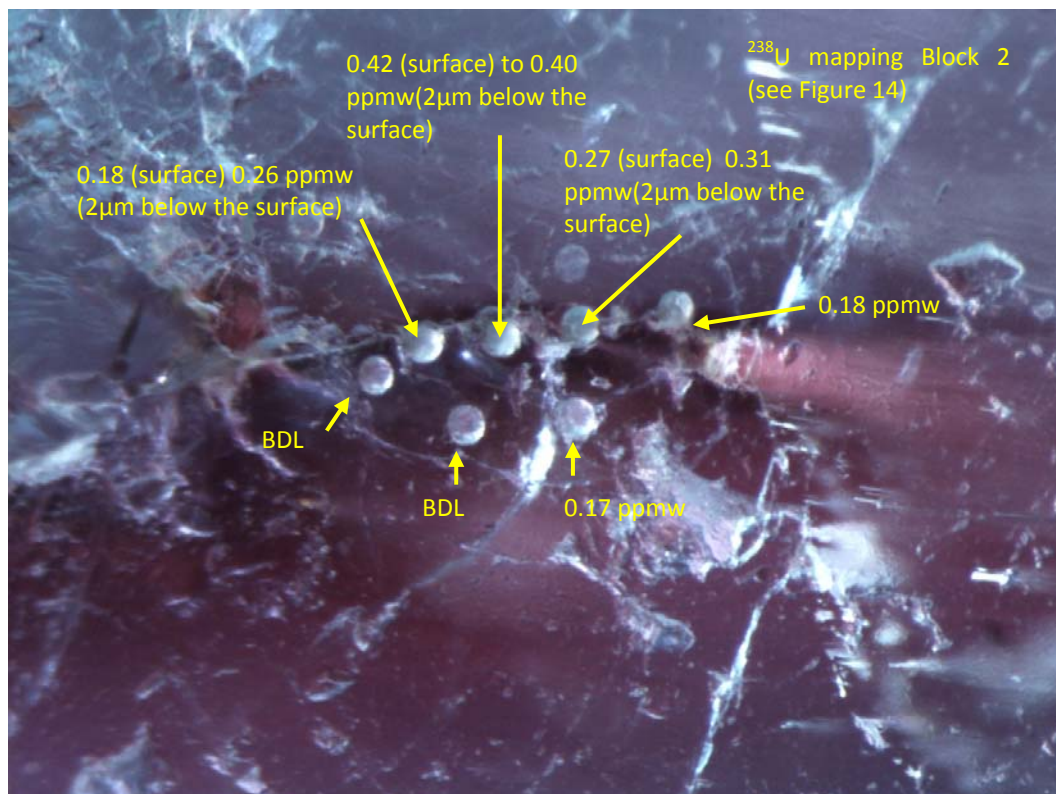


Figure 82: Enlarged photomicrograph of the ^{238}U mapping from Figure 80.

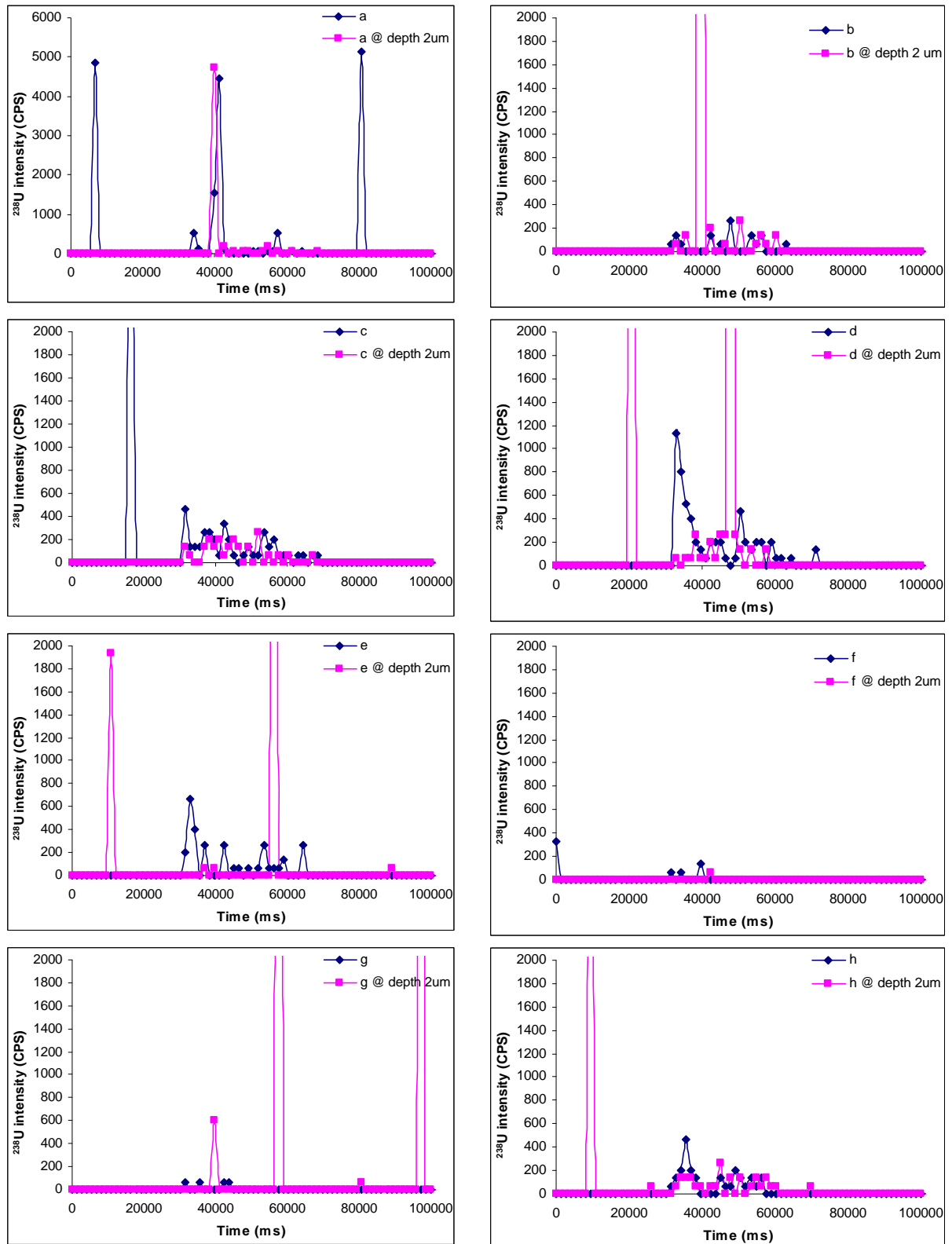


Figure 83: Photomicrograph of the spots analyzed by using LA-ICP-MS after the stone had been ground down 0.5 cm. Each spot was analyzed at the ground down surface (first number in the following pairs for each spot) and 2 μ m below the surface (second number in the following pairs for each spot).

Analysis of the fabricated surface

To reach within the unusual pinkish purple color zone and to determine that the results were not confined to the surface only, the stone was ground down in the area of a pinkish purple zone that was associated with a fracture (Figure 83), by approximately 0.5 cm and cleaned with acetone. The pinkish purple color zone was then analyzed along the fracture at the new ground down surface as well as 2 μ m below this; the analysis points are marked in Figure 83 as 'a' through to 'o'. The results show that only the analysis points within the pinkish purple zones contain ^{238}U , while areas away from the fracture and outside the color zone showed no ^{238}U concentrations. The ^{238}U concentrations for each analysis point in Figure 83 are recorded at the surface (first number in the following pairs for each spot) and 2 μ m below the surface (second number in the following pairs for each spot); BDL and 0.04 ppmw at spot a; BDL and 1.38 ppmw at spot b; BDL and 0.07 ppmw at spot c; 0.06 and 0.40 ppmw at spot d; 0.03 ppmw and BDL at spot e; BDL at spot f and g; 0.03 and BDL at spot h; 0.22 and 0.10 ppmw at spot i; 0.02, 0.02 and 0.01 ppmw at spot j; BDL at spot k; 0.32 and 0.43 at spot l; 0.02 and 0.01 ppmw at spot m; 0.04 and 0.08 ppmw at spot n; BDL and 0.04 ppmw at spot o.

The ^{238}U intensities for each analyzed point are set out in Figure 84 and the concentrations are shown in Table 2. It was also observed that the variation in ^{238}U partially correlated with the variation in ^{232}Th Figure 85.



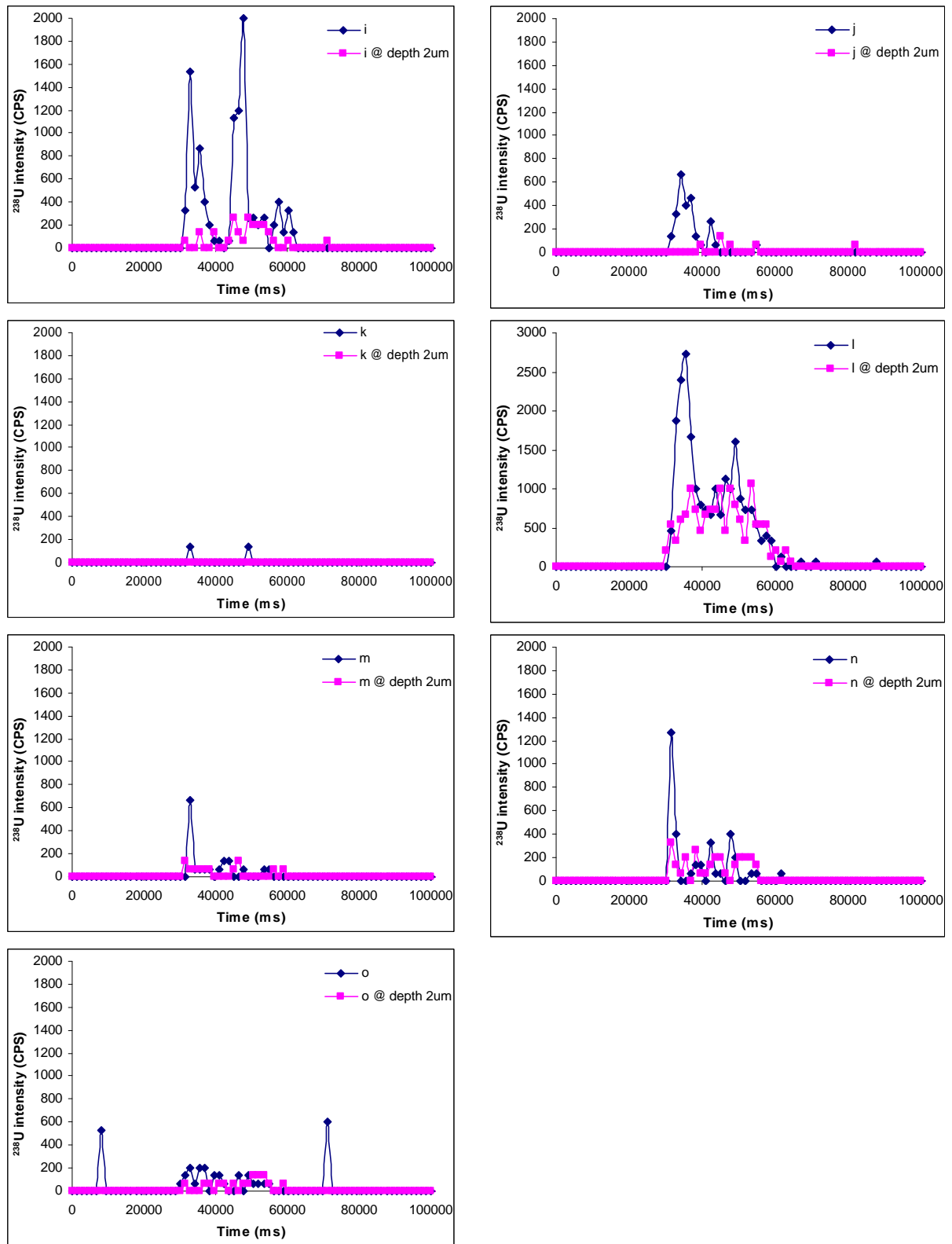


Figure 84. ^{238}U Intensity versus time on each spot in the pinkish purple colored fracture in the tourmaline in Figure 83 where blue and pink indicate laser spots on the ground down surface and 2 μm below the surface, respectively.

Table 2: ^{238}U and ^{232}Th concentrations in ppmw on the pinkish purple color fracture Figure 17.

Spot (s)	^{238}U (ppmw)		^{232}Th (ppmw)	
	Ground down surface	2 μm below the ground surface	Ground down surface	2 μm below the ground surface
a	BDL	0.04	0.05	0.06
b	0.06	1.38	0.03	0.05
c	BDL	0.07	0.07	0.09
d	0.06	0.40	0.04	0.05
e	0.03	BDL	BDL	BDL
f	BDL	BDL	0.01	BDL
g	BDL	BDL	0.01	0.01
h	0.03	BDL	0.04	0.03
i	0.22	0.10	0.03	0.04
j	0.02	0.02	0.01	0.04
k	BDL	BDL	0.01	0.01
l	0.32	0.43	0.49	0.58
m	0.02	0.01	0.02	0.01
n	0.04	0.08	0.04	0.05
o	BDL	0.04	0.04	0.04

Note: The laser-ablation parameters for this experiment were; 40 μm spot diameter, ~ 10 J/cm 2 laser fluence, 7 Hz repetition rate, and 25 second dwell time. NIST 610 and 612 glass reference material were used to calibrate and boron was used as internal standard. Boron was assumed as 3.26% for this tourmaline. Detection limit (BDL) was 0.01 ppmw for both ^{238}U and ^{232}Th .

Discussion

This simple one specimen study confirms that uranium and thorium were present within a pinkish purple colored fracture in a tourmaline and that these elements are confined to the areas close to the fracture and within the pinkish purple colored zone. These results tend to support the assumptions and conclusions of Koivula and Peretti et.al that these pinkish purple areas appear to be induced by radioactive materials (fluids) entering fractures and growth tubes in tourmaline.

Clearly more specimens need to be analyzed before a better understanding of the mechanisms involved is achieved, however it would appear that an alternative and more likely cause for these color concentrations in tourmaline has now been firmly established. Certainly the assumption that these color concentrations are produced artificially by one of the diffusion processes has been put to question and been found to be lacking in substance.

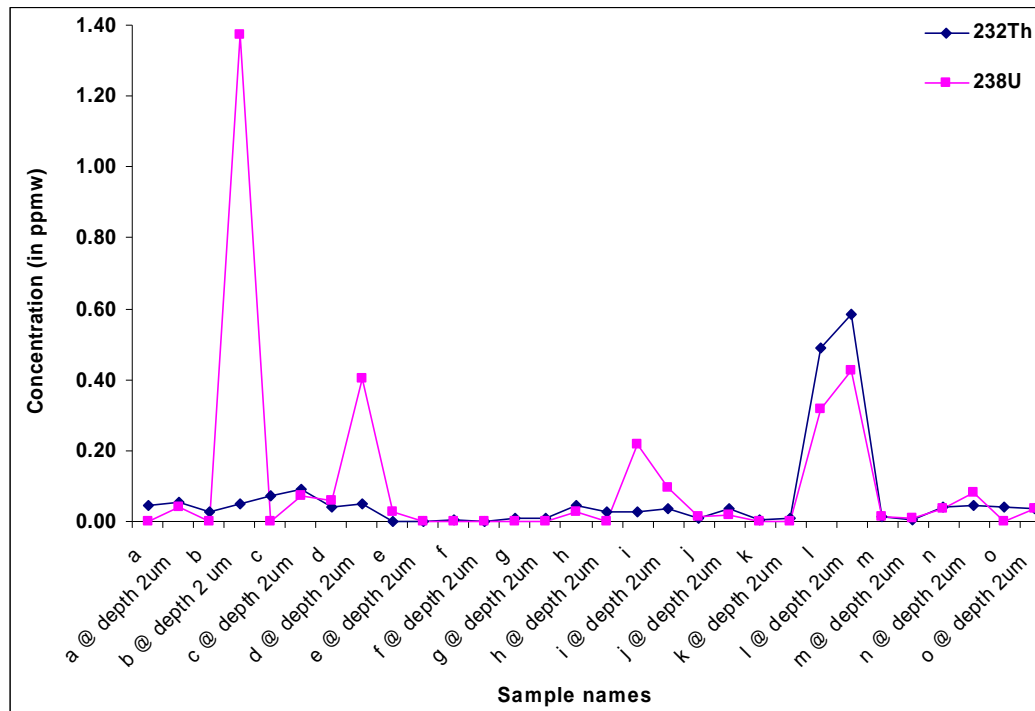


Figure 85: Variation in ²³²Th and ²³⁸U in pinkish purple colored fractures in this tourmaline.

Acknowledgements

Special thanks are due to several people and companies that continue to make this ongoing program possible. Richard Hughes for continued support and provision of specimens, Wuyi Wang and Andy Shen of GIA for support and critique, and Miranda Gems of Hong Kong for providing the majority of samples. Thank you.

References:

Abduriyim, A., Kitawaki, H., Furuya, M., Schwarz, D. (2006) Paraíba-type Copper-bearing Tourmaline from Brazil, Nigeria, and Mozambique: Chemical Fingerprinting by LA-ICP-MS. *Gems & Gemology*. 42. 1. 4-21

Abduriyim A., K. H., Furuya M., Schwarz D. (2006) "Paraiba" - type copper-bearing tourmaline from Brazil, Nigeria, and Mozambique: Chemical fingerprinting by LA-ICP-MS. *Gems & Gemology*. 42. 1. 4-20.

Emmett, J. L., Scarratt, K., F. McClure, S., Moses, T., Douthit, T.R., Hughes, R., Novak, S., Shigley, J.E., Wang, W., Bordelon, O., Kane, R.E. (2003) Berillium Diffusion of Ruby and Sapphire. *Gems & Gemology*. 39. 2.

Fritsch, E., Shigley, J. E., Rossman, G. R., Mercer, M. E., Muhlmeister, S. M. and Moon, M. (1990) Gem-quality cuprian-elbaite tourmalines from Sao Jose da Batalha, Paraiba, Brazil. *Gems and Gemology*. 26. 3. 189-205

GIT. (2009) Heating Experiment of Copper-Bearing Tourmaline and Some Interesting Features. Lab

Notes. http://www.git.or.th/eng/testing_center_en/lab_notes_en/glab_en/2008/heating_experiment_en.html. July 2009

James, R. (2009a) The Diffusion of Heavy Metals into Gemstones! Part I of III that will lead up to the ISG at Tucson 2009

Seminar! <http://www.yourgemologist.com/ISGForumsBoard/showthread.php?t=4152>. 22 March 2009

James, R. (2009b) The Diffusion of Heavy Metals into Gemstones: Pink Tourmaline! Part II of III that will lead up to the ISG at Tucson 2009

Seminar! <http://www.yourgemologist.com/ISGForumsBoard/showthread.php?t=4173>. 24 March 2009

James, R. (2009c) The Grain Boundary Diffusion: Understanding the Process! Part III of III that will lead up to the ISG at Tucson 2009

Seminar!! <http://www.yourgemologist.com/ISGForumsBoard/showthread.php?t=4185>. 24 March 2009

Kammerling, R. C. and Koivula, J. I. (1989) Thermal alteration of inclusions in "rutilated" topaz. *Gems and Gemology*. 25. 3. 165-167

Koivula J. I., N. K., Shen A. H-T., Owens P. (2009) Solution-generated pink color surrounding growth tubes and cracks in blue to blue-green copper-bearing tourmalines from Mozambique. *Gems & Gemology*. 45. 1. 44-47

Koivula, J. I. (1987) Goethite Inclusion Alteration during the Heat Conversion of Amethyst to Citrine. *Australian Gemmologist*. 16. 7.

Koivula, J. I. (2009) GIA reports pink color around growth tubes in Copper-Bearing Tourmalines results from natural irradiation. . GIA Insider.

<https://app.e2ma.net/app/view:CampaignPublic/id:13748.1679463988/rid:db0f385657d90d782d6bd72e97999b59#article1>. 24 March 2009

Laurs, B. M., Zwaan, J.C., Breeding, C.M., Simmons, W.B., Beaton, D., Rijdsdijk, K.F., Befi, R., Falste, A.U. . (2008) Copper-bearing (Paraíba-type) Tourmaline from Mozambique. *Gems & Gemology*. 44. 1. 4-30

LMHC. (2007) Information Sheet #6, Paraíba tourmaline. <http://www.giathai.net/pdf/IS6%20paraiba%20at%20April%2019%2007.pdf>. 24 March 2009

Palache, C., Berman, H., Frondel, C (1944), *The System of Mineralogy*, vol 1, John Wiley & Sons, New York

Peretti, A., Bieri, W.P., Reusser, E., Hametner, K., Gunther, D. (2009) Chemical Variations in Multicolored "Paraíba"-Type Tourmalines from Brazil and Mozambique: Implications for Origin and Authenticity Determination. *Contributions to Gemology*. 9. 46

Reddy, B. J., Frost, R.L., Martens, W.N., Wain, D.L., Kloprogge, J.T. . (2007) Spectroscopic characterization of Mn-rich tourmaline. *Vibrational Spectroscopy*. 44. 42-49

Wise, R. W. (2009) Drama In The Desert: ISG Seminar--A Dry Hole. <http://gemwiseblogspotcom.blogspot.com/search?updated-max=2009-02-28T12%3A13%3A00-05%3A00&max-results=1>. March 22 2009